

Supporting Information

Quadrupole moments determine crystal structures of organic semiconductors

Takehiko Mori

Department of Materials Science and Engineering, Institute of Science Tokyo, O-
okayama 2-12-1, Meguro-ku, Tokyo 152-8552, Japan. E-mail: mori.t@mac.titech.ac.jp

Parameters of intermolecular interaction

To define the molecular coordinates (X , Y , Z) (Fig. 1(h)), the molecular center (x_0 , y_0 , z_0) was estimated from the rectangular coordinates (x , y , z) of a molecule obtained from the reported crystal data. Then, six elements of the inertia,

$$\langle xx \rangle = \sum (x - x_0)^2, \quad \langle xy \rangle = \sum (x - x_0)(y - y_0), \quad \text{etc.} \quad (\text{S1})$$

were calculated. After the diagonalization of the 3×3 matrix, (X , Y , Z) were obtained by multiplying the eigenvectors to $(x - x_0, y - y_0, z - z_0)$. The resulting molecular coordinates, (X , Y , Z), were oriented along the molecular long, short, and vertical axes, respectively (Fig. 1(h)). The inertia was calculated from all non-hydrogen atoms, in which the alkyl groups and the substituents were not included. Then, the molecular long axis was unambiguously defined even when the molecule did not have the D_{2h} symmetry.

In the HB, θ -, γ -, and $P\pi$ -structures, the molecules were placed on inversion centers, and the molecular coordinates were obtained from the lattice constants and θ .¹³

$$\begin{aligned} Y_g &= \frac{a}{2} \sin \frac{\theta}{2} - \frac{b}{2} \cos \frac{\theta}{2} \\ Z_g &= \frac{a}{2} \cos \frac{\theta}{2} + \frac{b}{2} \sin \frac{\theta}{2} \\ X_s &= 0 \quad Y_s = b \cos \frac{\theta}{2} \end{aligned} \quad (\text{S2})$$

$$Z_s = b \sin \frac{\theta}{2} \quad \text{but } Z_s = 3.45 \text{ \AA} \text{ for } \theta > 90^\circ \quad (\text{S3})$$

Lattice constants were converted to $b < a < c$ (Fig. 1(a)), where b was the monoclinic unique axis, and c was the interlayer direction. The molecular width W was defined by the difference of the maximum and minimum Y coordinates appearing in the molecule (Fig. 1(h)). Usually, W comes from hydrogen atoms.

From the condition of molecular contact, the lattice constants were estimated from the molecular width $Y_0 = W + 1.9$ \AA and the molecular thickness $Z_0 = 3.45$ \AA.

$$a = Y_0 + Z_0 - (Y_0 - Z_0) \cos \theta \quad (\text{S4})$$

$$b = [Y_0 + Z_0 + (Y_0 - Z_0) \cos \theta] / 2 \quad (\text{S5})$$

These were cosine functions connecting $(a, b) = (2Z_0, Y_0)$ at $\theta = 0^\circ$ and $(2Y_0, Z_0)$ at $\theta = 180^\circ$.

The intermolecular energy was estimated according to the standard 6-exp potential,^{S1-S8}

$$V = \varepsilon \left[A \exp \left(-B \frac{r}{r_0} \right) - C \left(\frac{r_0}{r} \right)^6 \right] \quad (\text{S6})$$

where $A = 184000$, $B = 12$, and $C = 2.25 \text{ kJ } \text{\AA} \text{ mol}^{-1}$.^{S9} The parameters were taken from the MM3 force field (Table S1).^{13,S10} For interaction between different atoms, the geometrical average was used for ε , while the arithmetic average was used for r_0 . There were no reliable parameters for Se, but the values that gave slightly larger potentials than S were used. To this dispersion energy, electrostatic energy was added,^{S3-S5,S8}

$$V_{\text{stat}} = \frac{D\rho_i\rho_j}{r} \quad (\text{S7})$$

where $D = 1380 \text{ kJ } \text{\AA} \text{ mol}^{-1}$. Charges ρ_i calculated from the molecular orbitals scattered largely,¹³ and significantly depended on the estimation methods, hence the same charge was allotted to the same kind of atoms (Table S1). The opposite charge was allotted to the connecting carbon atoms so as to maintain the charge neutrality (Fig. S1). Charges on N and S were either positive or negative depending on the environments, so the average values were adopted. The results reproduced the reported charges well.¹⁵ Usually, electrostatic energy between various atoms canceled each other, and the total electrostatic contribution was less than 10% of the total intermolecular energy.^{13,14}

Table S1 Force-field parameters^{S10}

Atom	ε (kJ mol ⁻¹)	r_0 (Å)	Charge ρ_i
C	0.2343	3.92	–
H	0.0837	3.24	0.115
S	0.8452	4.30	0.07
O	0.2466	3.64	-0.30
N	0.1797	3.86	0.00
F	0.3135	3.42	-0.20
Se	1.8	4.30	0.07

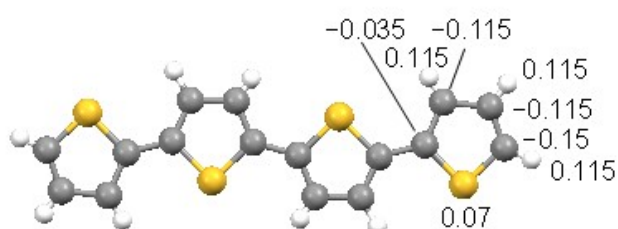


Fig. S1 Charges on 4T.

Quadrupole moments

Table S2 Quadrupole moments ($e \text{ \AA}^2$)

Compound		Q_{xx}	Q_{yy}	Q_{zz}	Compound		Q_{xx}	Q_{yy}	Q_{zz}
naphthalene	HB	3.80	3.31	-7.11	terrylene	SHB	10.53	9.45	-19.98
anthracene	HB	5.44	4.40	-9.83	pyrene	SHB	5.66	5.49	-11.16
tetracene	HB	7.66	5.69	-13.35	perylene	SHB	7.38	6.59	-13.97
pentacene	HB	9.79	5.93	-15.75	coronene	γ	8.14	7.78	-15.92
crysene	HB	7.21	5.66	-12.87	ovalene	γ	11.94	9.89	-21.83
picene	HB	8.96	7.01	-15.97	zethrene	γ	8.67	7.82	-16.49
2P	HB	5.11	3.79	-8.90	hexabenzocoronene	γ	15.05	14.81	-29.87
3P	HB	7.57	5.36	-12.92	peryllo thiophene	γ	10.55	3.03	-13.58
4P	HB	10.31	8.44	-18.74	bisanthrene	SHB, 0, γ	10.17	9.26	-19.43
PvPvP	HB	8.77	6.97	-15.74	tetra benzoanthracene	$P\pi$	11.47	10.51	-21.97
PvPvPvPvP	HB	19.62	9.19	-28.82	fluoranthene	HB	5.72	5.25	-10.97
AzAzAz	HB	13.44	9.48	-22.93	acenaphtho acenaphthyrene	γ	8.94	7.49	-16.43
4T	HB	16.16	1.01	-17.17	benzofluoranthene	$P\pi$	7.51	6.50	-14.01
C4-4T	HB	33.09	-8.63	-24.46	dithiapyrene	0	13.48	-3.40	-10.09
6T	HB	29.01	-2.41	-26.60	TT	0	8.07	-1.75	-6.32
8T	HB	44.32	-3.97	-40.35	TTT	0	11.25	-2.72	-8.53
TT-TT	HB	10.24	2.52	-12.76	TTTT	0	15.48	-4.51	-10.97
T-TT-T	HB	16.34	1.19	-17.54	TTTTT	0	19.76	-5.81	-13.95
P-T-P	HB	11.71	0.78	-12.49	TTT-TTT	0	25.91	-6.68	-19.22
P-2T-P	HB	15.31	3.08	-18.39	T-TTT-T	0	23.68	-3.61	-20.07
P-6T-P	HB	40.58	0.64	-41.22	C6T-TTT-T	HB	42.83	-15.66	-27.17
2P2T2P	HB	23.29	5.30	-28.59	dibenzodithia pentalene	0	11.69	-2.57	-9.12
2P3T2P	HB	29.05	5.08	-34.13	dithiapyrene	0	13.48	-3.40	-10.09
2P4T2P	HB	36.82	3.04	-39.85	PSeSeP	HB	11.15	1.46	-12.61
PTTP	HB	11.82	0.31	-12.12	C8PSeSeP	0	20.12	-5.35	-14.76
C3PTTP	HB	17.02	-3.22	-13.80	C8PSeSeP0v		19.06	-2.65	-16.41
C8PTTP -P	HB	18.98	-2.02	-16.96	C8PSeSeP0h		22.82	-7.05	-15.78
C8PTTP	HB	22.11	-5.39	-16.72	C10PSeSeP	Ila	23.40	-7.83	-15.57
C8PTTP0v		19.55	-5.31	-14.24	C12PSeSeP	0	18.70	-5.99	-12.71
C8PTTP0h		21.59	-4.17	-17.42	C14PSeSeP	Ila	23.75	-9.34	-14.41
C10PTTP	HB	20.10	-5.44	-14.67	4O	III	17.93	-2.44	-15.48
C12PTTP	HB	19.83	-5.66	-14.17	6O	HB	28.05	-3.91	-24.14
PTTPPP (DNTT)	HB	16.66	1.30	-17.96	POOP	$P\pi$	8.94	-0.51	-8.43
PPPTTPPP (DATT)	HB	22.05	2.92	-24.97	PPOPP	$P\pi$	9.83	4.78	-14.61
PPTPP	HB	11.45	2.65	-14.10	PQP	$P\pi$	19.73	-14.03	-5.69
PTPTP	HB	16.06	-0.92	-15.14	PPQPP	Ib	32.33	-17.07	-15.27
C4PTPTP	Ib	24.92	-5.63	-19.29	PQPQP	Ib	42.69	-32.73	-9.96
C10PTPTP	0	24.86	-8.23	-16.63	PZQZP	Ib	46.44	-33.05	-13.39
C10PTPTP-P	HB	22.36	-4.30	-18.06	PP-Tz-PP	HB	25.35	-4.86	-20.50
PTTTP	HB	15.89	-1.11	-14.78	PP-TzTz-PP	HB	32.02	-6.85	-25.17
C6PTTTP	0	28.55	-9.82	-18.73	2T-TzTz-2T	Ib	39.85	-12.17	-27.69
PTT-TTP	0	21.10	-3.32	-17.78	PZP	Stack?	15.39	-5.80	-9.59
PPTPTPP	0	21.29	-0.70	-20.59	PZPP	$P\pi$	19.03	-5.85	-13.18
C10PPTPTPP	HB	35.74	-10.84	-24.90	PPZPP	III	24.61	-7.06	-17.55
PTT-TTP	0	21.47	-2.86	-18.61	YZPP	Ib	21.85	-11.36	-10.49
PTPPT'P	0	11.87	4.36	-16.23	Bd'Bd	Ib	-3.88	4.12	-0.27
PNP	HB	-9.42	9.97	-0.56	BdQBd	Ib	2.71	-18.86	16.15
PNNP	HB	-2.09	13.24	-11.14	Bd'QBd'	Ib	8.41	-9.58	1.17
PPNPP	HB	1.98	11.86	-13.84	σY -Bd- σY	Ib	19.86	-7.77	-12.09
P-PNP-P	HB	5.77	11.05	-16.82	mY -Bd- mY	0+Ib	-2.29	1.60	0.68
PAP	HB	-0.29	0.41	10.12	pY -Bd- pY	Ib	-23.24	11.26	11.98
PAPP	HB	-1.62	12.83	-11.21	NC-2P-CN	Ib	-48.87	31.22	17.65
PPAPP	HB	-3.64	14.98	-11.34	TTF	$P\pi$	16.28	-5.17	-11.11
(CH ₃) ₂ N-2P-N(CH ₃) ₂	HB	26.08	-4.94	-21.14	DBTTF	0	21.60	-3.64	-17.96
					BDF	$P\pi$	-31.50	22.28	9.22
					BFD	$P\pi$	24.39	-17.42	-6.97
					TdZTd	HB	13.67	-16.72	3.06

Table S2 (continued) Quadrupole moments ($e \text{ \AA}^2$)

Compound		Q_{xx}	Q_{yy}	Q_{zz}	Compound		Q_{xx}	Q_{yy}	Q_{zz}
fP-T-fP	θ	-8.61	-0.23	8.84	PDI	Ib	-33.26	15.77	17.49
fP-2T-fP	Ib	-14.03	5.66	8.38	C5PDI	Ib	-16.78	6.46	10.32
fP-3T-fP	Ib	-20.50	9.74	10.76	C4PDI	$\text{P}\pi$	-18.92	-7.99	10.93
fP-4T-fP	Ib	-32.96	23.76	9.20	6fT	III	-6.22	-5.05	11.27
fP-PPP-fP	Ib	-19.90	2.23	17.67	fPPP	γ	-4.01	-6.41	10.42
fP-perylene-fP	HB	-21.43	12.62	8.81	fPPPP	γ	-8.03	-9.32	17.35
fP-2O-fP	Ib	11.54	-15.80	4.26	α -2CH ₃ T-TPT	HB	19.33	12.16	-31.49
2T-2fP-2T	θ	47.99	-20.79	-27.20	4CH ₃ T-perylene	Ib	46.29	-21.27	-25.02
T-fP-2T-fP-T	$\text{P}\pi$	39.6	-17.73	-21.87	4CH ₃ T-perylene	Ib	50.02	-25.03	-24.99
NDI	BW	-9.42	-1.47	10.88	2CH ₃ T-PPPP	IIb	29.05	-5.98	-23.07
C4NDI	BW	1.48	-8.03	6.55	4CH ₃ T-PPPP	IIb	41.67	-8.71	-32.96
C6NDI	BW	14.99	-14.96	-0.02	TIPS-pentacene	Ib	13.10	8.64	-21.74
Cy6NDI	BW	8.16	-11.61	3.46	TMS-pentacene	Ib	16.97	6.33	-23.30
Cy6PPPDI	BW	11.60	-15.09	3.49	Rubrene	$\text{P}\pi$	-8.73	14.76	-6.03
Cy6PZPDI	BW	25.62	-27.06	1.45					

Table S3 Quadrupole moments ($e \text{ \AA}^2$) with considerable Q_{xy}

Compound		Q_{xx}	Q_{yy}	Q_{zz}	Q_{xy}
TPT	HB	7.26	1.15	-8.41	-7.48
TPPT	HB	7.45	1.70	-9.16	11.05
TPPPT	HB	8.93	4.81	-13.74	11.72
TPTPT	$\text{P}\pi$	-2.76	-13.68	16.44	0.72
TTPTT	III	18.91	-4.62	-14.29	-0.05
C6TTPTT	Ib	31.93	-11.67	-20.27	8.37
CSPTTP	Ib	6.51	2.38	-8.88	-7.91
TPTTP	SHB	15.07	-0.55	-14.52	5.09
OPO	HB	7.59	-0.41	-7.17	-6.44
C8POOP	Ia	15.98	-4.36	-11.61	-7.82
4O	III	16.65	-1.17	-15.48	4.94
<i>o</i> Y-PPP- <i>o</i> Y	HB+Ib	24.30	-3.60	-20.70	-20.13
<i>p</i> Y-PPP- <i>p</i> Y	Ib	-29.27	16.96	12.30	-27.37
H ₂ phthalocyanine	γ	14.03	12.71	-26.75	9.51
indigo	III	20.07	-8.90	-11.18	-7.80
quinacridone	I,II,III	26.47	-14.98	-11.49	-28.08
CH ₃ O-2P-OCH ₃	HB	10.47	2.02	-12.49	-16.78
CH ₃ O-4P-OCH ₃	HB	29.05	-2.70	-26.35	27.57
CH ₃ O-2P-2T-2P-OCH ₃	HB	45.40	-3.71	-41.69	-36.42
CH ₃ O-2P-3T-2P-OCH ₃	HB	35.58	7.39	-42.97	0.00
CH ₃ OP-TzTz-POCH ₃	θ	42.26	-16.29	-25.97	-26.15
CF ₃ P-PPP-PCF ₃	HB	-23.41	11.98	11.43	11.43
CF ₃ P-2T-PCF ₃	HB	-43.42	34.86	8.56	8.56
CF ₃ P-T-Bd-T-PCF ₃	HB+Ia	-59.16	47.01	12.15	12.15
CF ₃ P-2Tz'-PCF ₃	θ	-30.07	22.72	7.35	9.28
CF ₃ P-2Tz-PCF ₃	Ib	-30.07	22.72	7.35	7.35
CF ₃ P-TzTz-PCF ₃	Ib	-28.77	21.51	7.26	7.26
CF ₃ P-T-TzTz-T-PCF ₃	Ib	-48.36	34.13	14.22	14.22
CF ₃ P-Tz-TzTz-Tz-PCF ₃	Ib	-38.92	24.44	14.48	14.48
CF ₃ P-Tz'-TzTz-Tz'-PCF ₃	Ib	-26.50	19.25	7.25	-14.26
CF ₃ P-PQP-PCF ₃	Ib	-32.94	17.47	15.48	-16.42
CF ₃ P-T-PQP-T-PCF ₃	Ib	-44.43	31.07	13.35	16.64
CF ₃ P-Tz-PQP-Tz-PCF ₃	Ib	-46.40	25.91	20.49	20.49
α -2CH ₃ T-TPT	HB	5.71	5.46	-11.17	-18.65
β -2CH ₃ T-TPT	$\text{P}\pi$	20.53	-4.46	-16.07	-16.64
β -2CH ₃ T-SePSe	θ	27.91	-10.57	-17.33	-4.22
β -2CH ₃ T-TPPT	$\text{P}\pi$	-7.49	4.37	3.12	-12.67
β -2CH ₃ T-TPPP	$\text{P}\pi$	37.58	-13.07	-24.51	7.95
β -2CH ₃ T-TTTT	$\text{P}\pi$	35.55	-15.73	-19.82	-10.06

Quadrupole moments are estimated by the DFT calculation in the B3LYP level with 6-31G basis set on Gaussian 16 (Table S2 and S3).³⁸ Quadrupole moments are defined as

$$Q_{xx} = \sum_i \rho_i x_i x_i, \quad Q_{yy} = \sum_i \rho_i y_i y_i, \quad Q_{zz} = \sum_i \rho_i z_i z_i \quad (S8)$$

for diagonal cases, where ρ_i designates charge distribution coming from the molecular orbitals, and the integration is for the whole molecule. As a primitive example, it is convenient to consider a point charge on atoms. For CO₂, when the charge on O is -0.89 and the C–O distance is 1.16 Å, the quadrupole moment is -2.395 e Å² (1 e Å² = 1 Debye Å = 16×10⁻⁴⁰ C m²). Aromatic hydrocarbons have positive Q_{xx} and Q_{yy} coming from C^{δ-}–H^{δ+} (Fig. 3(b) inset). Raw Q_{xx} , Q_{yy} , and Q_{zz} calculated from molecular orbitals are negative because the electron cloud spreads over the molecule. However, the traceless values have the electrostatic meaning, and these values are discussed in this paper. When the molecular coordinates are used, the nondiagonal components (Q_{xy} , Q_{yz} , and Q_{zx}) are practically zero due to the molecular symmetry. Table S3 lists compounds with significant Q_{xy} values.

By extending the molecule, (Q_{xx} , Q_{yy}) increases as shown in Fig. 4(a) and (b). The slopes are (ΔQ_{xx} , ΔQ_{yy}) = (2.0, 0.9 e Å²) for P in acenes, (2.6, 2.3 e Å²) for nP, (13, -1.8 e Å²) for 2T in the 4T – 6T – 8T series, and (6.5, -0.9 e Å²) for T in the 2P-2T-2P – 2P-3T-2P – 2P-4T-2P series. The slope goes down when the T number increases, but the PTTP – PPTTP – PPTTPP series slightly goes up, (5, 1 e Å²), because the P content increases. All these compounds have the HB structure. The fused thiophenes, namely the TT – TTT – TTTT series form a slope of (3.9, -1.4 e Å²), and this slope constructs the border to the stacking structure (Fig. 4(a) and (b)).

Structural parameters of fundamental aromatic compounds

Table S4 – S6 lists fundamental aromatic compounds not investigated in my previous paper,^{13,14} and actual organic semiconductors. Oligothiophenes and oligo selenophenes such as 2Se and 4Se have the HB structure (Table 4), but fused compounds, TT and SeSe even with only two rings, form the θ-structure (Table 5).^{S11} The Y_g , Z_g , Y_s , and Z_s values satisfy the ordinary HB relations (eqns (S2)-(S5)) as shown in Fig. S2.

In general, anthracene-containing compounds have the HB structure. Recently, oligo(p-phenylenevinylene) derivatives have been extensively studied due to the high quantum yields of the photoluminescence.⁵⁵⁻⁵⁷ PvPvP (Fig. S3), PvPvPvP, and PvPvPvPvP have the HB structure, but one and half molecules are crystallographically independent because two thirds of X_g is as large as 4.9 Å. PvPPPvP does not have an ordinary HB structure owing to the large Y_g (4.26 Å) associated with the unusually small $\theta = 38.1^\circ$. However, C5PvPPPvP forms an ordinary HB structure.

Phenyl naphthodithiophene (Fig. S3) and the 2P analogue (2P-naphthodithiophene-2P) have the HB structure. The small $\theta = 28^\circ$ – 26° means an intermediate to the BW structure, but the considerably tilted P parts form a more normal HB ($\theta = 85^\circ$). The thiophene analogue (T-naphthodithiophene-T)

has the θ -structure (θ -P π in Table S5).

PPTT, a part of dinaphthothienothiophene (DNTT: PPTTPP), and the several related compounds have the HB structure (Table S4). PTTP-PPP-PTTP is a molecule containing two BTBT units.

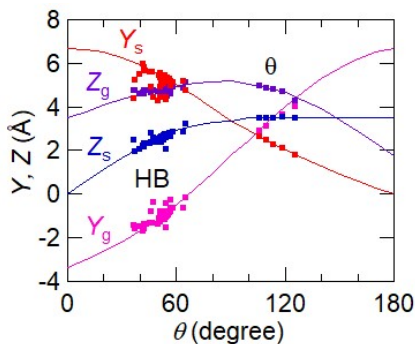


Fig. S2 Intermolecular geometry of HB and θ -structure compounds in Table S4 and S5 with the standard relations of the HB structure (eqns (S2)-(S5)).

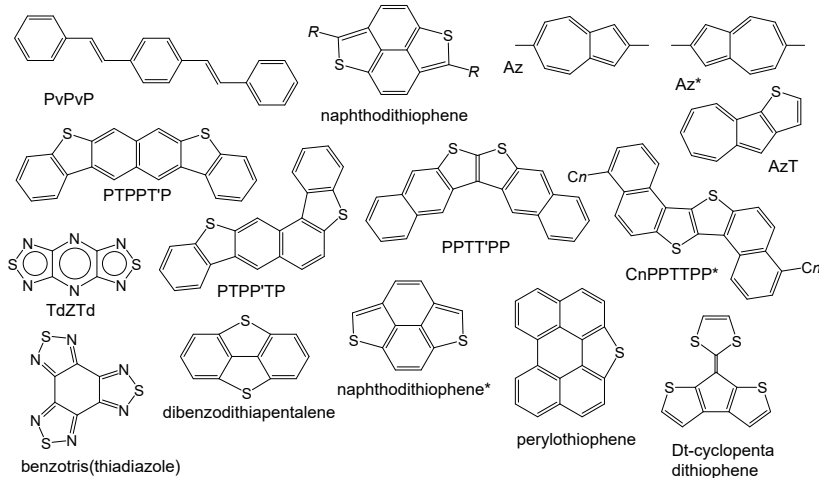


Fig. S3 Molecular structures of compounds in Table S4 and S5.

Azulene derivatives have been investigated as organic semiconductors.⁶⁰ Since azulene (Az) has peripheral hydrogens, the parent azulene as well as the oligomers have the HB structure (Table S5). As shown in Fig. 4(a), Az-Az-Az has the typical Q_{xx} and Q_{yy} values of the HB structure. Katagiri has demonstrated that Az trimers show ambipolar transistor properties,^{58,59} but the dominant carrier changes depending on the Az orientation (distinguished using Az* in Fig. S3) due to the localization of the highest occupied molecular orbital (HOMO) and the lowest unoccupied molecular orbital (LUMO).

Table S4 Structure parameters of HB compounds containing various units

Compound ^a	μ_{max} (cm ² V ⁻¹ s ⁻¹) ^a	θ (°)	W (Å)	X_g (Å)	Y_g (Å)	Z_g (Å)	V_g (kJ mol ⁻¹)	X_s (Å)	Y_s (Å)	Z_s (Å)	V_s (kJ mol ⁻¹)	CCDC	Ref
HB													
2Se		60.5	4.65	1.34	-0.88	4.86	-16.86	0.80	5.16	3.04	-13.05	144304	S12
4Se		64.8	4.82	1.34	-0.14	4.83	-39.23	2.74	4.54	2.97	-36.67	142022	S13
P-PPP-P	(34)	50.5	5.90	0.43	-1.23	4.64	-51.23	0.81	5.60	2.64	-31.46	1044209	S14
C1P-PPP-P	2.40	48.4	5.96	0.62	-1.17	4.66	-57.96	1.28	5.42	2.45	-40.71	1982542	S15
C2P-PPP-P	1.57	51.1	5.88	0.49	-1.02	4.77	-62.24	0.97	5.38	2.57	-43.67	1442079	S16
C3P-PPP-P	1.34	53.2	6.02	0.61	-0.99	4.71	-66.60	1.26	5.22	2.63	-47.60	1982543	S15
CH ₃ OP-PPP-POCH ₃	2.96	41.2	10.49	0.11	-1.58	4.56	-63.01	0.73	5.72	2.16	-42.43	1442078	S16
CH ₃ SP-PPP-POCH ₃ ^b	0.12	47.4	11.38	0.32	-1.34	4.68	-62.79	1.13	5.49	2.23	-45.49	1442077	S16
					5.93	0.12	-1.05	4.77	-62.95	0.57	5.41	2.62	-46.34
PP-PPP-PP	2.1	48.8	5.76	0.40	-1.13	4.65	-68.42	0.56	5.42	2.46	-50.69	1901585	S17
PvPvP ^b		61.5	4.42	4.90	-0.16	4.40	-36.08	2.92	4.60	2.78	-31.17	2031306	55
		62.8		1.44	-0.40	4.59	-40.35	3.41	4.48	2.57	-34.01		
PPvPvPP		60.3	4.70	1.40	-0.41	4.64	-69.15	2.90	4.62	2.69	-55.71	1009831	56
PvPvPvP ^b	0.12	53.2	4.49	4.85	-0.52	4.38	-53.91	2.64	4.61	2.48	-44.92	2034951	57
	0.11 e	61.4		1.30	-0.64	4.56	-60.42	3.51	4.55	2.18	-56.47		
PvPvPvPvP		58.0	4.53	4.91	-0.23	4.42	-70.77	2.72	4.68	2.69	-59.56	129139	S18
		64.4		1.35	-0.51	4.64	-76.26	3.54	4.43	2.40	-72.78		
PvPPvPvP	(4.3)	38.1	7.35	0.39	4.26	4.58	-38.20	0.46	5.30	2.53	-34.74	977506	S19
C5PvPPvPvP	1.28	51.0	9.42	0.32	-1.08	4.51	-91.45	0.46	5.27	2.50	-61.15	621869	S20
PvBZvP ^b		48.8	7.21	0.40	-1.78	4.72	-45.90	0.01	5.46	1.91	-39.99	1974596	S21
		54.1	7.52	6.48	-2.27	4.14	-31.99	0.22	5.03	2.85	-39.09		
		49.0	7.22	6.24	-2.46	4.39	-30.29	0.09	5.26	2.40	-38.66		
P-naphthodithiophene-P	0.057	28.0	9.00	2.81	-1.52	4.47	-51.19	6.55	4.56	1.82	-11.85	267032	S22
2P-naphthodithiophene-2P	0.036	25.8	6.80	0.68	-2.04	4.37	-83.62	10.64	6.39	1.49	-28.38	267031	S22
T-PPP-T (monoclinic)	(0.029)	49.7	5.84	3.96	-1.17	4.63	-43.64	0.03	5.41	2.51	-33.26	1988561	S23
T-PPP-T (orthorhombic)	0.063	52.5	5.84	1.34	-1.00	4.69	-45.71	1.34	5.32	2.64	-34.86	265820	S24
C6-2T-PPP-2T		46.1	9.68	5.01	-1.26	4.57	-87.47	0.04	5.37	2.29	-73.85	1956922	S25
P-T-P		49.8	4.84	0.09	-1.01	4.72	-31.03	0.01	5.28	2.45	-22.86	1264781	S26
P-2T-P		56.6	4.84	1.15	-0.62	4.71	-43.74	0.25	5.01	2.75	-32.28	2259365	S27
P-6T-P		62.7	6.04	1.20	-0.27	4.76	-80.43	2.53	4.61	2.84	-71.12	232986	S29
PTTTTPP	2.1	46.6	8.13	1.08	-1.08	4.66	-58.96	0.66	5.62	2.44	-35.53	2103738	S30
P'PTTTTPP'	4.2×10 ⁻³	46.5	5.99	0.29	-1.48	4.79	-59.20	0.63	5.98	2.57	-36.44	2103739	S30
PTTT		56.1	5.09	0.11	-0.78	4.71	-25.89	0.40	5.09	2.73	-18.60	2056747	S31
PPPTT	0.012	52.3	5.07	0.56	-0.98	4.65	-30.52	1.21	5.18	2.56	-26.48	1577634	S32
PPTT-T		54.6	6.74	3.66	-0.24	4.67	-39.93	1.58	4.96	2.69	-27.29	2056748	S31
PPPTT-T		36.8	5.83	1.33	-1.78	4.58	-46.95	0.22	5.87	1.96	-31.37	2056749	S31
PTTT-P	0.70	51.5	5.26	0.25	-0.94	4.82	-38.16	0.44	5.36	2.58	-24.65	916026	S32
PTTT-2P ^b	0.11	53.6	4.78	0.42	-0.89	4.73	-53.72	1.18	5.19	2.61	-34.77	916023	S32
		4.80	0.75	-0.84	4.73	-54.06	1.21	5.17	2.64	-34.88			
PTTT-PP ^b	0.088	50.2	5.26	0.01	-1.08	4.69	-47.79	0.60	5.32	2.59	-30.47	916024	S32
		49.9	6.43	0.19	-1.07	4.67	-46.18	0.05	5.36	2.67	-30.42		
PPP-TTT-PPP	1.26	42.3	5.65	0.31	-1.43	4.57	-78.30	0.02	5.56	2.15	-51.30	2237416	S33
PTTP-PPP-PTTP	0.22	53.3	5.81	0.04	-0.94	4.79	-88.72	0.08	5.28	2.65	-62.50	1909445	S34
P-PNP-P		51.3	5.61	2.53	-0.87	4.53	-43.19	0.29	5.17	2.49	-38.62	705361	S35
OPO		47.5	4.79	0.33	-1.17	4.50	-16.12	1.46	5.13	2.33	-14.04	2125893	10
2P-2O-2P ^c	0.27/0.013e	53.6	6.06	12.12	-0.94	5.34	-30.76	0.96	5.07	2.49	-54.25	922141	S36
T-2O-T		61.4	5.40	0.21	-0.32	4.82	-31.43	0.03	4.70	2.79	-30.11	927826	S37
POP-PPP-POP	3.0	48.9	5.81	0.33	-1.16	4.64	-76.06	0.61	5.42	2.46	-53.77	1506173	S38
CH ₃ O-2P-OCH ₃		64.6	4.11	1.22	-0.46	4.59	-31.89	2.36	4.81	3.01	-22.01	604799	S39
CH ₃ O-4P-OCH ₃		64.5	4.03	1.25	-0.39	4.67	-60.07	2.47	4.77	3.00	-43.28	700242	S40
CH ₃ O-2P-2T-2P-OCH ₃		51.8	5.29	0.77	-0.97	4.57	-81.54	1.53	5.16	2.50	-60.95	883460	S41
CH ₃ O-2P-3T-2P-OCH ₃		49.0	6.88	0.00	-1.06	4.67	-96.28	0.00	5.28	2.41	-69.72	1991924	S42
(CH ₃) ₂ N-2P-N(CH ₃) ₂		61.2	4.14	7.76	-0.51	4.79	-19.91	2.25	4.92	2.93	-25.41	1278586	S43
mY-4T-mY ^d		53.7	4.83	2.34	-0.81	4.65	-46.06	0.08	5.10	2.58	-30.08	627860	S44
PP-Tz-PP		40.9	5.43	0.47	-1.22	3.49	-54.55	1.67	5.52	2.15	-28.15	2179267	S45
PP-TzTz-PP	0.042	46.7	5.49	0.38	-1.25	4.60	-52.67	1.13	5.34	2.30	-35.28	609620	S46
TdZTd		56.2	2.95	1.73	-0.75	4.28	-13.03	2.29	4.75	2.64	-9.62	1163438	S47
N-P-2T-P-N		50.4	5.19	2.59	-1.14	4.61	-63.07	0.97	5.15	2.41	-49.10	783089	S48
<i>o</i> Y-PPP- <i>o</i> Y ^e	10 ⁻⁵	54.5	8.38	0.26	-1.08	4.69	-47.50	0.36	5.53	2.85	-23.99	1439492	S49
fP-PPP-fP B	(2.65 e)	45.2	7.79	1.59	-1.20	4.66	-70.89	3.75	5.21	2.44	-13.76	2164678	S50
fP-PPP-fP B'		44.9	7.77	1.61	-1.21	4.64	-71.26	3.78	5.20	2.41	-12.99	2164677	S50
fP-perylene-fP	0.12/1.89	61.4	6.51	0.89	0.43	5.65	-48.50	0.31	5.51	3.28	-63.11	2178552	S50

^a Field-effect hole mobility unless indicated as “e” for electron mobility. ^b Two or three crystallographically independent molecules. ^cFurane (O) oligomers usually do not form the HB structure. An interpenetrated HB with large $X_g = 12.12$ Å is formed, where the 2O part does not have the HB packing. ^dmY: m-pyridine. ^eoY: o-pyridine.

:

Table S5 Structure parameters of HB Az compounds and compounds containing various units with HB, θ -, γ -, and SHB structures

Compound ^a	μ_{\max} (cm ² V ⁻¹ s ⁻¹) ^a	θ (°)	W(Å)	X _g (Å)	Y _g (Å)	Z _g (Å)	V _g (kJ mol ⁻¹)	X _s (Å)	Y _s (Å)	Z _s (Å)	V _s (kJ mol ⁻¹)	CCDC	Ref	
HB														
CF ₃ P-PPP-PCF ₃		58.1	9.13	3.45	1.21	5.56	-40.89	8.89	1.62	3.00	-40.90	252391	S51	
CF ₃ P-2T-PCF ₃	0.18 e	54.7	5.21	1.11	-0.78	4.70	-48.91	2.29	5.06	2.64	-38.58	1427491	S52	
CF ₃ P-T-Z-T-PCF ₃ ^{b,c}	8.3×10 ⁻⁴ e	69.1	9.18	1.15	-1.56	4.16	-57.88	4.90	1.71	3.35	-60.92	629009	S53	
			8.23	0.10	4.48	4.85	-29.84	1.05	6.05	0.69	-46.15			
CF ₃ P-T-BZ-T-PCF ₃ ^d		49.2	6.45	1.20	-1.47	4.39	-67.98	0.47	5.57	2.56	-54.04	1423924	S54	
CF ₃ P-T-Bd-T-PCF ₃ ^d	0.19 e	50.3	5.99	1.20	-1.07	4.48	-61.64	0.38	5.21	2.73	-49.16	1423925	S54	
Azulene (Az)		56.0	5.32	1.21	-0.92	4.70	-13.52	0.49	5.22	2.74	-12.93	1104286	S55	
AzT		55.8	5.06	0.00	-0.87	4.96	-21.36	0.10	5.32	2.82	-17.52	1111622	S56	
Az-Az-Az	0.29 e	53.4	5.04	1.23	-0.99	4.58	-59.53	0.03	5.25	2.64	-41.45	942762	58	
Az-Az-Az* ^b	1.32	54.5	5.05	1.03	-0.94	4.64	-57.48	0.39	5.24	2.71	-41.53	1505217	59	
			5.06					0.34	5.26	2.70	-41.47			
Az-Az*-Az ^b	0.31 e	51.6	4.96	0.26	-1.03	4.52	-60.05	1.34	5.21	2.53	-39.86	1505219	59	
			4.96					1.32	5.23	2.51	-39.50			
Az*-Az-Az ^b	0.15 e	51.4	5.01	0.49	-1.08	4.59	-60.41	1.15	5.34	2.60	-39.62	1505218	59	
			5.01					1.12	5.36	2.56	-39.90			
Az-2T-Az* ^e	0.024	51.9	5.20	0.97	-0.92	4.65	-58.72	1.97	5.15	2.51	-44.24	884333	S57	
Az-TT-Az* ^b	0.05	54.1	5.07	1.73	-0.87	4.62	-52.76	1.02	5.16	2.60	-39.45	884334	S57	
			5.09					1.07	5.12	2.66	-39.73			
Az*-Td-Az	0.0065 e	50.3	5.66	0.50	-1.20	4.63	-45.62	0.91	5.28	2.52	-30.63	2179265	S45	
Az-Td-Az* ^b		46.8	4.92	1.38	-1.17	4.62	-44.74	0.31	5.43	2.34	-31.84	2179266	S45	
			4.92					0.21	5.43	2.36	-31.72			
θ														
TT		141.2	4.60	2.66	3.52	3.73	-7.10	3.89	2.10	4.24	-7.81	1270552	S58	
SeSe		137.7	4.59	2.65	3.51	3.91	-7.19	3.80	2.25	4.19	-10.01	1257025	S59	
PTTTTP		127.2	6.06	0.44	4.23	4.28	-17.62	0.28	1.71	3.49	-62.41	2092479	S30	
PTPPT'P	7×10 ⁻⁵	137.2	6.09	1.82	5.20	4.17	-21.63	0.70	1.47	3.55	-67.09	856943	S60	
dibenzodithiaphentalene		126.2	4.96	5.02	3.87	4.40	-8.45	0.14	1.80	3.57	-36.90	1190865	S61	
dibenzoselenathiaphentalene		124.5	5.12	4.97	3.73	4.58	-10.66	0.25	1.88	3.60	-45.07	1299929	S61	
NCP-2T-PCN		154.0	5.16	5.66	5.17	3.02	-18.15	10.96	1.12	3.40	-31.29	613515	S62	
mY-Bd-mY ^f		144.1	5.47	8.23	3.24	3.57	-10.62	0.49	1.26	3.56	-52.70	241256	S63	
CH ₃ OP-TzTz-POCH ₃		128.4	4.15	10.25	3.29	4.00	-15.49	0.83	1.74	3.48	-59.66	609618	S45	
CF ₃ P-2Tz'-PCF ₃ ^b		148.0	4.69	3.45	4.61	3.40	-26.23	2.80	0.98	3.63	-71.81	291640	S64	
			4.80					2.87	1.04	3.56	-72.92			
fP-T-fP		150.6	5.35	0.61	5.63	3.79	-15.79	4.28	1.40	3.53	-47.69	619630	S65	
2T-2fP-2T ^e	4×10 ⁻⁵	136.6	5.73	0.94	4.96	3.64	-20.96	1.14	1.38	3.56	-60.95	207398	S66	
θ-Pπ														
T-naphthodithiophene-T		127.8	8.83	0.77	5.95	5.11	-17.50	0.04	1.73	3.53	-74.45	178734	S67	
γ														
PPTT'PP A ^b		74.7	6.77	0.69	2.37	6.90	-23.02	4.22	1.91	3.45	-56.62	1523533	S68	
		72.3	6.78	1.30	0.99	7.19	-25.47	4.06	2.29	3.40	-55.70			
PPTT'PP B ^g	5.1×10 ⁻⁵	129.3	6.78	1.64	6.70	5.35	-6.18	0.10	1.65	3.49	-67.03	1523534	S68	
PTPPT'P ^b	7×10 ⁻⁵	152.2	7.50	1.23	7.44	3.81	-14.74	3.24	0.18	3.47	-68.23	856944	S32	
PPPTT'PPP														
perlylo thiophene	2.2×10 ⁻⁴	156.9	8.29	10.43	0.52	1.51	-22.39	0.68	1.40	3.56	-91.49	1523532	S68	
Dt-cyclopentadithiophene	0.8	100.3	6.89	2.88	0.33	3.47	-56.45	7.93	1.12	3.61	-11.35	129291	S69	
naphidot di thiophene* ^e		126.3	7.84	6.48	1.48	5.58	-12.40	1.80	0.17	3.57	-49.39	1230716	S70	
benzotris(thiadiazole)		119.8	6.41	6.01	0.71	5.89	-6.25	2.07	0.10	3.57	-38.63	1171543	S67	
perfluoranthracene		136.5	5.85	0.00	7.24	2.89	-8.82	0.00	1.35	3.39	-28.63	1517238	S71	
perfluoropentacene	0.11 e	88.5	5.47	1.23	2.67	5.57	-18.68	0.16	3.24	3.24	-50.55	2089979	62	
H ₂ phthalocyanine	(0.3) ^h	88.8	12.51	4.65	3.76	8.28	-19.55	3.29	0.40	3.38	-85.60	234729	63	
SHB									3.1/2					
PTTTP	0.24	86.7	4.85	0.40	0.58	5.25	-28.67	1.38	0.09	3.50	-55.84	1968888	S73	
					0.90	2.94	4.92	-20.90	1.25	5.69	2.63	-19.29		
dibenzodiselenapentalene		73.6	5.21	0.42	0.33	5.72	-18.70	2.70	0.15	3.47	-37.89	1299927	S61	
					4.12	2.70	5.56	-10.31	4.61	4.63	3.43	-14.60		

^a Field-effect hole mobility unless indicated as “e” for electron mobility. ^b Two crystallographically independent molecules. ^c The molecular long axes are non-parallel. ^d Stacking pattern appears alternately with the HB pattern (Table S7). ^e The half molecule is interpenetrated because the 2fP unit is non-planar. ^f mY: m-pyridine. Alternate patterns of θ and parallel. ^g Another polymorph. ^h CuPc single crystal.

Table S6 Structure parameters of stacking compounds containing various units

Compound ^a	μ_{\max} (cm ² V ⁻¹ s ⁻¹) ^a	θ (°)	X_g (Å)	Y_g (Å)	Z_g (Å)	V_g (kJ mol ⁻¹)	X_s (Å)	Y_s (Å)	Z_s (Å)	V_s (kJ mol ⁻¹)	CCDC	Ref	
Stack Ia (BW)						s1				s2			
perfluoroanthracene			1.79	3.09	3.24	-48.69	3.69	5.07	2.79	-36.76	2089978	62	
perfluoropentacene (TF) ^b			0.05	3.13	3.22	-85.60	1.34	5.56	2.26	-30.89	918801	64	
			2.48	2.86	3.24	-79.05	1.36	5.19	2.74	-75.03			
isoindigo	0.0011/0.0028 e		1.45	3.74	3.20	-31.82					1180974	S74	
Stack Ib						s1				s2			
Az*-Td-Az ^c	0.0065e		1.02	1.47	3.65	-48.86	1.02	4.46	3.65	-45.62	2179265	S45	
2T-TzTz-2T	0.02		2.98	1.47	3.79	-66.20	1.51	4.33	2.83	-53.30	223086	S75	
CF ₃ P-2Tz-PCF ₃	1.83 e		9.01	2.28	3.37	-43.45	12.57	4.18	3.37	-19.28	291639	S63	
CF ₃ P-T-TzTz-T-PCF ₃	0.26 e		2.40	1.19	3.61	-74.62	1.64	4.22	2.83	-65.36	1427490	S52	
CF ₃ P-Tz-TzTz-Tz-PCF ₃ ^b	0.12 e		1.70	0.44	3.49	-96.47	0.59	6.03	1.93	-32.29	648764	S76	
			9.37	0.69	3.64	-69.47	1.15	5.56	1.65	-28.15			
CF ₃ P-Tz'-TzTz-Tz'-PCF ₃ ^b	3×10 ⁻⁴ e		3.03	1.33	3.46	-81.85	1.29	5.63	1.48	-38.12	648765	S76	
			2.82	1.55	3.55	-83.14	4.42	5.11	1.68	-31.03			
CF ₃ P-PQP-PCF ₃	7×10 ⁻⁴ e		2.27	0.51	3.59	-93.02	4.74	7.26	3.22	-23.69	709632	S77	
CF ₃ P-T-PQP-T-PCF ₃	0.02 e		3.35	0.01	3.31	-134.47	6.03	0.54	3.56	-102.23 ^p	709633	S77	
CF ₃ P-Tz-PQP-Tz-PCF ₃ ^a	0.074 e		0.46	1.66	3.37	-113.30	8.70	3.82	3.24	-83.60	709634	S77	
			1.34	5.52	2.79	-58.56	9.67	7.61	3.02	-34.90			
F3P-TzTz-PF3 ^d	0.93		1.27	3.40	-51.60	1.04	5.48	2.39	-29.44	609619	S46		
<i>o</i> Y-Bd- <i>o</i> Y ^e	0.44		1.29	3.52	-52.63	1.71	7.49	0.08	-13.07	241255	S63		
<i>p</i> Y-Bd- <i>p</i> Y ^e	1.25		1.70	3.80	-42.43	6.64	7.28	0.68	-13.60	241257	S63		
<i>p</i> Y-PPP- <i>p</i> Y	0.05		1.05	0.87	3.50	-67.40	10.11	2.41	3.63	-13.19	2166838	S78	
Bd'Bd'	1.90		1.72	3.32	-32.10	3.31	6.68	2.32	-4.32	1517239	S71		
BdQBd	0.00		1.73	3.39	-46.75	7.86	4.31	2.83	-12.65	1400306	S79		
Bd'QBD'	0.25		1.73	3.38	-51.31	5.94	6.89	3.09	-12.36	1517243	S71		
fP-PPP-fP G	0.09		1.52	3.45	-69.33	1.14	5.76	2.64	-41.67	2164676	S50		
PTTT-fP	6.2×10 ⁻⁶ e		5.28	1.19	3.47	-44.92	0.84	5.66	2.42	-19.21	916028	S34	
fP-2T-fP	10 ⁻⁵ e	5.6	5.41	1.10	3.70	-60.74	1.06	6.34	2.13	-16.75	619629	S65	
fP-3T-fP ^b	0.003 e		4.42	1.70	3.51	-75.14	0.48	5.59	2.29	-37.49	619628	S65	
			5.37	0.38	3.64	-72.41							
fP-4T-fP ^b	0.43 e		11.92	1.07	3.62	-54.38	1.45	5.82	2.18	-17.36	207396	S66	
			14.31	0.82	3.44	-45.34							
fP-2O-fP			3.72	0.16	3.27	-73.76	8.45	6.65	2.44	-12.08	1893115	S80	
Stack IIb (Pπ)													
T-fP-2T-fP-T	0.01		87.9	3.47	1.08	3.50	-113.54	0.30	5.88	2.11	-49.53 ^p	207397	S66
BDF			118.7	2.37	0.99	3.33	-25.15	2.19	4.21	2.81	-20.21 ^p	2181371	65
BFD			72.7	4.51	0.09	3.32	-36.46	2.34	4.04	3.07	-28.86 ^p	2224811	66
Stack III											V_g		
PPZPP	83.6		3.77	0.59	3.41	-49.54	3.03	6.10	0.57	-11.50	2334205	S81	
Bz	133.4		1.49	0.19	3.49	-17.31	0.16	6.15	1.67	-4.07	1109160	S82	
Tz-Bz-Tz	87.9		3.38	1.21	3.40	-44.84	3.30	6.26	0.94	-10.24	265881	S83	
CF ₃ P-TzTz-PCF ₃	65.1		5.44	1.15	3.55	-53.48	4.18	5.02	1.90	-12.04	1427489	S52	
6fT	83.3		3.78	1.23	3.54	-93.96	2.52	5.78	3.31	-16.45	164573	S84	

^a Field-effect hole mobility unless indicated as “e” for electron mobility. ^b Two crystallographically independent molecules. ^c The Td part has the stacking (Ib) structure, but the Az part is HB (Table S5). ^d F3P: 2,4,5-trifluorophenyl. ^e oY: *o*-pyridine, *p*Y: *p*-pyridine. Bd is stack, but Y is HB.

Table S7 Supplementary structure parameters of compounds with various units

Compound	<i>b</i> (Å)	θ (°)	<i>X</i> (Å)	<i>Y</i> (Å)	<i>Z</i> (Å)	<i>V</i> (kJ mol ⁻¹)	CCDC
HB							
PPTT	7.5957	56.3	0.01	0.76	4.71	-24.64	2056747
PPTT-T	5.857	54.6	2.43	1.22	3.49	-36.62	2056748
TdZTd	6.847	43.0	4.44	2.18	2.56	-12.01	1163438
CF ₃ P-T-BZ-T-PCF ₃ ^a	6.142	49.2	3.83	3.77	3.57	-78.62 ^a	1423924
CF ₃ P-T-Bd-T-PCF ₃ ^a	5.898	50.3	3.41	3.44	3.70	-76.49 ^a	1423925
Az-Td-Az*	5.9224	46.5	9.70	1.79	4.64	-24.60	2179266
		47.0	9.96	1.56	4.72	-23.12	
θ							
dibenzodithiapentalene	4.00	126.2	5.07	5.18	2.42	-10.36 ^p	1190865
dibenzoselenathiapentalene	4.07	124.5	5.14	5.24	2.38	12.34 ^p	1299929
<i>m</i> Y-Bd- <i>m</i> Y	3.8113	144.1	3.71	6.55	4.00	-8.94 ^a	241256
γ							
PPTT'PP A	5.7734	73.4	1.38	8.28	1.94	-14.58	1523533
		72.3	5.85	5.99	1.94	-15.33	
PPTT'PP B	3.8657		4.33	5.76	2.47	-29.20 ^p	1523534
PTPP'TP	4.748	152.2	8.00	6.09	4.76	-9.08 ^g	856944
			6.03	7.14	3.22	-13.58 ^p	
		152.2	5.42	3.50	6.28	-10.03 ^g	
			0.41	7.91	2.11	-13.02 ^p	
perythiophene	4.5252	100.3	1.07	8.16	1.79	-11.83 ^g	129291
naphthodithiophene*	4.1280	119.8	4.03	6.36	2.16	-10.25 ^p	1171543
Stack Ia (BW)						<i>V</i> _s	
isoindigo	6.400/2		2.91	7.48	0.00	-6.89	1180974
Stack Ib						<i>V</i> _s	
Az*-Td-Az	5.922		0.00	5.92	0.00	-30.63	2179265
2T-TzTz-2T	6.0540		1.46	5.80	0.96	-22.32	223086
CF ₃ P-2Tz-PCF ₃	6.736		3.57	6.46	0.00	-15.74	291639
CF ₃ P-T-TzTz-T-PCF ₃	8.1828		1.34	5.82	0.95	-30.49	1427490
CF ₃ P-Tz-TzTz-Tz-PCF ₃	5.914		1.11	5.59	1.56	-27.03	648764
CF ₃ P-PQP-PCF ₃	8.1535		2.47	7.77	0.38	-25.11	709632
CF ₃ P-T-PQP-T-PCF ₃	7.7033		3.13	4.38	3.02	-61.21	709633
CF ₃ PP-Tz-PQP-Tz-PCF ₃	12.2445		1.34	5.52	2.79	-58.57	709634
F3P-TzTz-PF3	3.744		0.11	6.76	1.00	-19.73	609619
<i>o</i> Y-Bd- <i>o</i> Y	3.7763		2.15	6.20	3.44	-12.82	241255
<i>p</i> Y-Bd- <i>p</i> Y	7.3213/2		1.10	2.56	3.47	-40.50	241257
<i>p</i> Y-PPP- <i>p</i> Y	3.7587		11.16	3.28	0.12	-11.79	2166838
PTTT-fP			6.12	6.85	1.05	-12.36	916028
fP-2T-fP	7.106/2		6.70	5.49	1.27	-15.59	619629
Stack IIb (Pπ)		<i>V</i> _s				<i>V</i> _c	
T-fP-2T-fP-T	5.0431	-21.90	15.16	1.16	11.02	-8.50	207397
BDF	4.2114	-13.32	7.95	2.55	3.03	-5.03	2181371
BFD	5.5998	-9.81	5.31	1.58	2.54	-9.01	2224811
Stack III		θ				<i>V</i> _c	
Bz	3.803	1.6	6.25	2.52	2.54	-3.61	1109160
CF ₃ P-TzTz-PCF ₃	6.60		10.79	5.94	2.33	-10.56	1427489
6fT ^b	5.3230	83.3	14.08	0.54	10.86	-10.75	164573

^a Stacking (Ia) pattern *V*_s appears alternately with the HB (θ) pattern. ^b Pπ direction.

The ordinary PTPPTP has been known (probably HB),^{S85} but the slightly wider PTPPT'P (Fig. S3) has the θ -structure, though this compound has positive Q_{yy} (Table S2). PTTP'TP is even wider, and the two polymorphs have the γ -structure. PPTT'PP is an isomer of DNTT (PPTTPP), but owing to the large width, this molecule as well as PPPTT'PPP have a γ -structure. In the θ - and γ - structures, Z_s corresponds to the interplanar spacing. Alkyl PPTTPP* (Fig. S3) forms stacking structures (Table 2), and shows excellent transistor properties.⁹⁴

TdZTd is a molecule which does not have any hydrogen atoms (Fig. S3). Though negative Q_{yy} suggests a stacking structure (Table S2), this compound has a significantly distorted HB structure (Table S4). Benzotris(thiadiazole) is another molecule not having hydrogen atoms, which forms a γ -structure with large θ (Table S5). Dibenzodithiapentalene (Fig. S3) and the mono-seleno analogue have the θ -structure (Fig. 4(a)), but the di-seleno analogue has a SHB structure (Table S5).

PP-Tz-PP and PP-TzTz-PP maintain the HB structure due to the naphthalene moieties; the comparatively small Q_{yy} values around $-5 \text{ e } \text{\AA}^2$ (Table S1) is agreeable with the HB structure (Fig. 4(b)), because they are located above the pale blue TTT θ line. These molecules are basically planar, but $\theta = 40.9$ and 46.7° are small. It is noteworthy that 2T-TzTz-2T has a stacking (Ib) structure (Table S6) owing to the large Q_{yy} value of $-12 \text{ e } \text{\AA}^2$ (Fig. 4(b)).^{S75} The TzTz part does not have any hydrogen atoms, and forms an entirely parallel stack, though the tilted 2T part forms a HB structure ($\theta = 41^\circ$).

Compounds containing terminal CF_3P parts have negative Q_{yy} (Table S3), and usually have the stacking (Ib) structures (Table S6). Some have HB and θ -like patterns (Table S5), but $\text{CF}_3\text{P}-\text{PPP}-\text{PCF}_3$ is characterized by the large X_s , where the PPP part is HB, but the CF_3P part is stacked. $\text{CF}_3\text{P}-2\text{T}-\text{PCF}_3$ has the ordinary HB structure, but the molecular long axes of $\text{CF}_3\text{P}-\text{T}-\text{Z}-\text{T}-\text{PCF}_3$ are significantly tilted. $\text{CF}_3\text{P}-\text{T}-\text{BZ}-\text{T}-\text{PCF}_3$ and $\text{CF}_3\text{P}-\text{T}-\text{Bd}-\text{T}-\text{PCF}_3$ have an alternate pattern of the HB and stacking structures. $\text{CF}_3\text{P}-2\text{Tz}-\text{PCF}_3$ has a stacking structure (Table S6), but $\text{CF}_3\text{P}-2\text{Tz}'-\text{PCF}_3$ has a θ -structure (Table S5); Tz designates a compound with the N atoms situated outside, whereas Tz' with the N atoms inside. $\text{CH}_3\text{OP}-\text{TzTz}-\text{POCH}_3$ has a θ -structure (Table S5), but $X_g = 10.25 \text{ \AA}$ is large.

Perfluorophenyl (fP) containing compounds are located in the 2nd quadrant (Fig. 5(a)), where Q_{xx} is negative (Table S2). fP-T-fP has a θ -structure (Table S5), whereas fP-2T-fP, fP-3T-fP, and fP-4T-fP have the normal stacking (Ib) structure (Table S6). One of the fP groups in fP-2T-fP is not coplanar, and form a HB-like structure. T-fP-2T-fP-T has a $\text{P}\pi$ structure (Table S6) in agreement with the negative Q_{yy} (Fig. 4(b)). However, the fP parts are sometimes not coplanar to the remaining part. fP-PPP-fP has polymorphs (B, B', C, and G),^{S50} where the torsion angles between the P and fP parts are as large as 45° . The B and B' phases as well as fP-perylene-fP form the HB structure, in which the core and the fP parts independently form oppositely tilted HB structures. The G phase belongs to the stacking (Ib) structure, in which the PPP and fP parts are oppositely tilted as well.

In a similar way, *o*Y-Bd-*o*Y and *p*Y-Bd-*p*Y have a stacking (Ib) structure, but *m*Y-Bd-*m*Y has an alternate pattern of the θ - and stacking structures. These compounds have entirely different moments

depending on the *o*-, *m*-, and *p*-pyridine (Table S2). The *o*- and *p*-forms are correctly located in the 4th quadrant stacking structure region, and the small moments in the *m*-form are consistent with the θ -pattern. Q_{xy} is large in *oY*-PPP-*oY* and *pY*-PPP-*pY* (Table S3), but the former is in Region (8) and the latter is in Region (4). The PPP part in *oY*-PPP-*oY* is HB, but the *oY* part is stacked. The large positive Q_{xx} and small negative Q_{yy} (Table S3) agree with the HB structure. *pY*-PPP-*pY* appears in the 2nd quadrant in agreement with a stacking (Ib) structure of both the PPP and *pY* parts; PPP and *pY* are differently tilted, but both have the stacking structure.

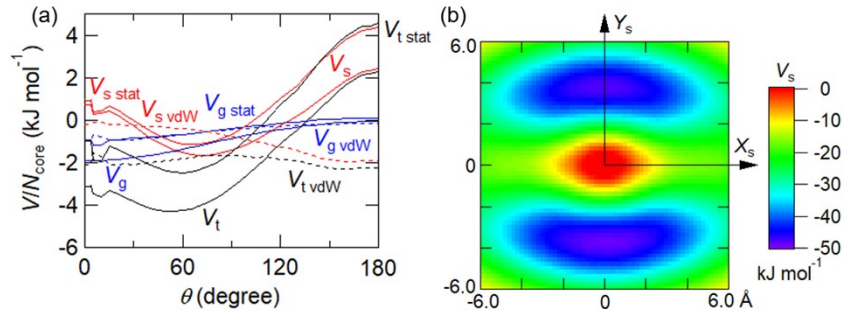


Fig. S4 (a) θ -dependent potential curve, and (b) $X_s Y_s$ -map in perfluoroanthracene (fPPP).

Structure parameters of alkyl compounds

Table S8 Structure parameters of HB and θ -structures in alkyl compounds

Compound ^a	$a \times b$ (Å ²)	θ (°)	X_g (Å)	Y_g (Å)	Z_g (Å)	V_g (kJ mol ⁻¹)	X_s (Å)	Y_s (Å)	Z_s (Å)	V_s (kJ mol ⁻¹)	
HB											
PTTP (BTBT)	46.50	56.4	0.17	-0.73	4.88	-26.66	0.32	5.16	2.77	-19.55	
C2PTTP	65.28	64.8	2.50	-0.15	5.14	-35.77	5.30	4.75	3.24	-22.76	
C8PTTP	46.70	56.4	0.23	-0.74	4.87	-69.99	0.51	5.20	2.79	-48.54	
C10PTTP	46.42	55.5	0.78	-0.78	4.84	-80.78	0.54	5.22	2.75	-54.94	
C12PTTP	45.39	55.2	0.24	-0.80	4.78	-93.31	0.51	5.18	2.71	-62.61	
mC2PTTP	55.08	56.1	0.39	-0.82	4.84	-32.58	0.20	5.31	2.83	-21.94	
mC3PTTP	45.81	54.6	7.33	-0.85	4.53	-26.21	0.58	5.34	2.75	-23.39	
mC4PTTP	48.13	58.1	0.59	-0.61	4.95	-36.83	0.30	5.13	2.85	-25.48	
mC9PTTP	47.34	63.9	0.58	-0.63	4.89	-45.19	0.63	5.21	2.86	-34.18	
C3PTTP-P	46.34	54.9	0.10	-0.80	4.93	-47.80	0.48	5.28	2.71	-30.96	
							0.50	5.28	2.71	-32.21	
C4PTTP-P	49.72	53.8	1.50	-1.04	4.77	-40.15	0.43	5.29	2.69	-26.08	
C5PTTP-P	47.54	51.5	0.25	-1.07	4.78	-55.25	0.39	5.47	2.64	-31.77	
C6PTTP-P	47.56	51.3	0.19	-1.07	4.78	-58.07	0.52	5.47	2.63	-33.51	
C8PTTP-P	47.50	51.0	0.07	-1.07	4.81	-63.53	0.23	5.49	2.62	-38.15	
C9PTTP-P	47.97	51.2	0.13	-1.08	4.81	-65.55	0.40	5.50	2.63	-39.24	
C10PTTP-P	46.91	50.2	0.41	-1.11	4.74	-69.55	0.41	5.46	2.56	-41.66	
C6PTTPP-P	47.31	51.2	0.30	-1.00	4.88	-63.86	0.71	5.43	2.61	-41.81	
C10'PTTP'-P	54.95	31.3	1.23	-4.17	4.49	-48.85	2.80	6.07	2.16	-31.50	
C10'PTTPP'-P	51.33	42.0	1.34	-1.59	4.63	-75.79	2.95	5.82	2.34	-33.80	
C5PTTP-PC1	54.44	54.2	6.66	-0.43	4.67	-47.17	0.43	5.30	2.72	-35.32	
C6PTTP-PC1	54.15	55.0	1.41	-0.97	4.79	-56.25	0.44	5.24	2.73	-41.55	
C7PTTP-PC1	54.42	55.0	1.41	-0.98	4.79	-56.05	0.44	5.25	2.74	-42.55	
C8PTTP-PC1	53.77	55.1	0.12	-0.96	4.79	-56.64	0.44	5.23	2.74	-46.84	
C9PTTP-PC1	46.12	53.9	0.11	-0.88	4.77	-68.80	0.25	4.37	2.09	-45.29	
C10PTTP-PC1	46.04	53.4	0.11	-0.87	4.85	-69.75	0.37	5.28	2.66	-46.72	
C11PTTP-PC1	46.22	54.3	0.11	-0.82	4.87	-71.07	0.40	5.25	2.70	-48.86	
C12PTTP-PC1	45.74	53.3	0.11	-0.88	4.83	-75.48	0.37	5.27	2.65	-50.45	
C13PTTP-PC1	46.49	54.6	0.16	-0.79	4.90	-77.89	0.47	5.24	2.71	-52.42	
C14PTTP-PC1	45.55	53.1	0.15	-0.89	4.81	-81.88	0.57	5.25	2.64	-54.07	
mC8PTTPP	47.42	54.0	0.17	-0.85	4.84	-57.91	0.80	5.31	2.71	-39.61	
			54.0	0.85	-0.85	5.00	-48.75	0.47	5.34	2.73	-39.75
mC8PPTTP	47.30	53.8	0.21	-0.87	4.83	-53.75	0.79	5.31	2.69	-36.27	
			53.8	0.52	-0.90	4.86	-54.31	0.82	5.30	2.71	-36.26
mC8'PTTPP	48.47	54.9	0.16	-0.83	4.85	-55.04	0.69	5.34	2.78	-40.42	
			0.60	-0.89	4.87	-54.84	0.72	5.34	2.76	-40.62	
mC8'PPTTP	48.47	53.2	0.46	-1.04	4.76	-53.33	0.27	5.44	2.77	-37.52	
			0.73	-1.12	4.86	-50.04	0.26	5.44	2.77	-37.50	
C6'PTTPT-P	50.41	54.3	4.53	-1.51	4.97	-41.82	8.57	4.46	2.63	-40.00	
			46.9	7.17	-0.36	4.78	-55.45				
			50.6	1.08	-0.79	4.83	-58.34				
C10'PTTPT-P	50.12	51.3	1.20	-1.10	4.75	-59.08	6.65	5.05	2.40	-34.10	
			46.1	5.47	-0.76	4.69	-45.96	6.58	4.92	2.81	-40.09
			49.7	0.88	-1.36	4.74	-64.73	1.23	4.29	2.41	-60.13
			36.8	0.95	-1.59	4.75	-58.19	6.74	5.27	1.97	-25.68
			36.0	5.16	-1.42	4.79	-46.06	2.94	4.43	2.51	-46.58
			39.4	1.28	-1.47	4.63	-70.16	6.49	5.53	2.10	-25.68
C6'PTTPT-P	48.06	53.4	0.15	-0.97	4.87	-59.45	0.38	5.45	2.73	-41.47	
			0.22	-0.99	4.86	-59.26	0.24	5.47	2.69	-41.64	
C10'PTTPT-P	47.83	52.9	0.92	-0.92	4.89	-70.78	0.40	5.41	2.72	-48.45	
			0.23	-0.98	4.85	-68.95	0.25	5.45	2.68	-48.09	
PPTTPP (DNTT)	47.40	51.1	1.36	-1.27	4.79	-45.00	0.58	5.58	2.61	-30.65	
C10PPTTPP	45.66	51.1	0.43	-1.03	4.71	-100.27	0.89	5.35	2.56	-63.41	
PTPTP	56.05	56.5	5.52	-0.72	4.64	-26.96	0.13	5.20	2.79	-26.29	
C10PTPTP-P	47.88	51.0	0.22	-1.10	4.81	-75.22	0.36	5.53	2.63	-46.89	
C10PPTPTP	47.24	46.2	0.18	-1.30	4.75	-106.57	0.41	5.62	2.40	-68.53	
PPTPP	48.07	41.1	0.59	-1.68	4.67	-38.95	0.22	5.98	2.24	-24.76	
C10PPTPP	47.56	42.2	1.70	-1.36	4.75	-92.04	0.23	5.67	2.19	-58.11	
C6'PPTPP	48.35	46.1	0.00	-1.29	4.77	-69.31	0.00	5.62	2.39	-47.44	
C10'PPTPP	47.56	45.3	0.00	-1.31	4.75	-91.03	0.00	5.62	2.34	-61.12	
TPPPT	45.98	51.7	0.36	-0.96	4.62	-36.80	1.50	5.14	2.52	-29.61	
C1TPPPT	52.04	51.1	2.02	-0.89	4.60	-43.51	4.29	4.96	2.53	-30.67	

Table S8 (continued) Structure parameters of HB and θ -structures in alkyl compounds

Compound ^a	$a \times b$ (\AA^2)	θ ($^\circ$)	X_g (\AA)	Y_g (\AA)	Z_g (\AA)	V_g (kJ mol^{-1})	X_s (\AA)	Y_s (\AA)	Z_s (\AA)	V_s (kJ mol^{-1})
P-2T-P ^a	45.44	56.6	0.93	-0.79	4.73	-44.25	0.30	5.05	2.68	-32.70
			1.15	-0.62	4.71	-43.74	0.25	5.01	2.75	-32.28
C2P-2T-P	52.17	52.5	2.61	-0.96	4.60	-53.84	0.08	5.14	2.53	-38.39
C6P-2T-P	52.55	52.9	2.64	-0.89	4.67	-64.19	0.09	5.07	2.52	-61.02
T-PPP-T ^a										
C6T-PPP-T	43.38	50.1	0.11	-1.09	4.59	-81.01	0.65	5.27	2.48	-56.12
C6-2T-PPP-2T		46.1	5.01	-1.26	4.57	-87.47	0.04	5.37	2.29	-73.85
P-TTT-P	46.85	56.5	0.02	-1.54	4.52	-46.76	0.02	5.58	1.97	-25.08
C8P-TTT-P	42.69	40.1	0.00	-1.48	4.44	-91.94	0.00	5.47	1.99	-50.42
C12P-TTT-P	43.21	40.1	0.00	-1.48	4.48	-114.54	0.00	5.49	2.00	-64.70
C8PP-TTT-PP	43.95	41.1	0.00	-1.46	4.51	-111.77	0.00	5.53	2.07	-66.42
4T	51.39	55.3	2.31	-0.86	4.70	-38.52	0.18	5.09	2.67	-28.71
C4-4T	47.44	61.3	1.24	-0.32	4.79	-60.89	4.64	4.64	2.82	-48.47
C6-4T	47.27	61.8	1.20	-0.29	4.78	-67.42	2.55	4.66	2.90	-51.31
C6T-TTT-T ^b	42.37	57.8	2.20	-0.49	4.80	-75.83	0.20	4.95	2.73	-47.95
						15.85	0.40	4.10		-52.08 ^b
C7T-TTT-T ^b	39.48	58.8	1.25	-0.50	4.69	-77.68	0.09	4.80	2.71	-53.57
						18.62	1.20	4.83		-46.69 ^b
C10TPPTP*	47.23	34.1	0.43	-4.30	4.94	-50.18	0.27	5.69	2.19	-46.95
PSeSeP	50.73	62.7	0.38	-0.41	5.15	-27.21	0.38	5.13	3.13	-20.18
θ										
PTPTP		125.2	5.19	4.04	4.32	-16.50	0.00	1.81	3.50	-53.92
C10PTPTP	46.48	109.1	0.16	3.15	4.89	-60.63	0.07	2.49	3.50	-116.12
C6PTTP	45.69	118.4	0.00	3.65	4.71	-41.08	0.00	2.11	3.54	-90.02
C8PSeSeP	46.85	113.5	0.50	3.51	4.81	-41.35	0.02	2.30	3.50	-99.26
C12PSeSeP	47.06	105.5	0.06	2.95	4.97	-62.00	0.39	2.64	3.50	-118.75

^a P-2T-P: 2259365,^{S86} T-PPP-T: 1988561.^{S87} ^b Stacking pattern alternately appears with the HB pattern.**Table S9** Structure parameters of stacking structures in alkyl compounds

Compound	W (\AA)	X_{s2} (\AA)	Y_{s2} (\AA)	Z_{s2} (\AA)	V_{s2} (kJ mol^{-1})	X_s (\AA)	Y_s (\AA)	Z_s (\AA)	V_s (kJ mol^{-1})
Stack Ia (BW)									
C8POOP	(4.71)	1.99	4.18	3.02	-74.04	1.03	6.39	0.32	-38.58
Stack Ib									
C12TPT		0.18	5.32	2.53	-63.27	1.44	6.49	1.14	-55.73
C8TOPOT		5.88	5.00	2.70	-22.53	2.05	6.28	0.82	-43.95
β -C10TTT		0.79	8.28	3.88	-4.44	8.03	6.48	0.35	-5.92
C3PTTP	4.67	3.33	6.28	2.23	-22.36	6.32	6.53	1.36	-16.25
C4PTTP	4.66	3.58	6.36	2.29	-27.66	6.53	6.55	1.29	-17.50
C5PTTP	4.55	3.74	6.26	2.33	-32.83	6.68	6.40	1.26	-19.20
C4PTPTP	6.47	6.88	6.12	2.34	-28.47	9.92	6.14	1.09	-16.55
C6TTPTT		0.44	5.98	2.24	-39.38	3.36	6.84	1.40	-43.50
C4PPTTPP*	7.04	3.33	6.76	2.53	-34.61	6.54	7.62	0.96	-20.62
C6PPTTPP*	7.27	0.64	6.62	2.79	-30.47	7.12	7.22	0.71	-23.33
C8PPTTPP*	7.04	5.48	6.65	2.90	-35.23	8.54	7.53	0.59	-25.55
C10PPTTPP*	7.05	3.28	6.30	3.21	-38.05	13.71	7.23	0.34	-34.91
Stack IIb (P π)									
C10PSeSeP		0.21	4.72	3.03	-53.10	5.57	7.30	0.60	-49.33
C14PSeSeP		0.51	4.61	3.08	-72.31	6.63	6.36	0.56	-74.70

Table S8 includes the unsubstituted compounds when the structure is the same as the alkyl compounds.¹³ Different cases are listed in Table S10. $X_s = 0 \text{ \AA}$ is universally observed in monoclinic crystals,¹³ but $X_g \sim 0 \text{ \AA}$ is characteristic of PTTP (BTBT).

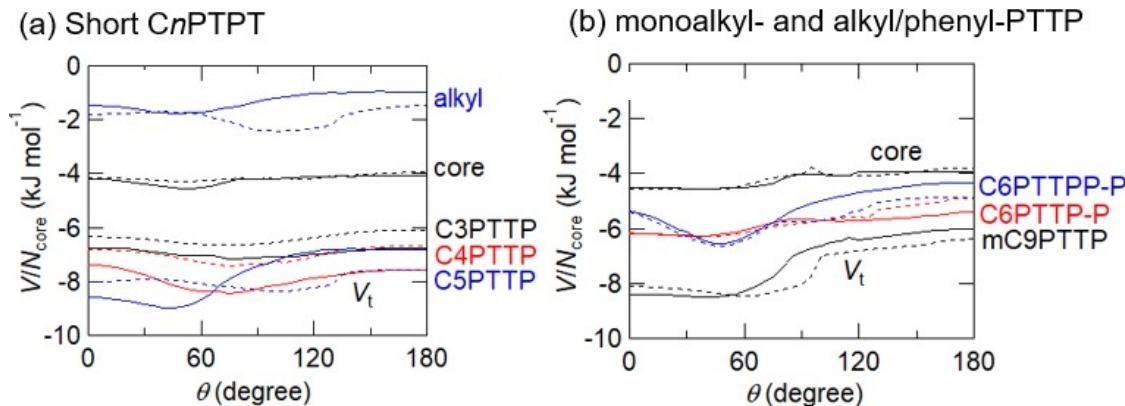


Fig. S5 θ -diagrams of (a) short alkyl, and (b) monoalkyl- and alkyl/phenyl-PTTP with vertical (solid) and horizontal (dashed) alkyl chains.

In short alkyl chains in Fig. S5(a), the alkyl chains are actually vertical, but the actual molecular packing is not HB but stacking. The contribution of the alkyl part is smaller than that of the core part. BTBT (PTTP) is located on the border between the HB and stacking structures.^{13,14} Short alkyl chains move it slightly to stabilize the stacking structure. By contrast, dinaphthothienothiophene (DNTT = PTTTPP) entirely prefers the HB structure due to the peripheral phenyl hydrogens.

In the θ -diagrams (Fig. 9 and S5), the BW structure corresponds to the $\theta = 0^\circ$ limit, but the core molecules are vertical.¹³ Therefore, the BW compounds are associated with the horizontal alkyl chains ($\varphi_2 = 0^\circ$). In Table 2, the first four compounds with comparatively large Y_{s1} have horizontal alkyl chains with $\varphi_2 = 0^\circ$. In the stacked molecules (Table 2), the alkyl chain is either horizontal ($\varphi_2 = 0^\circ$) or vertical ($\varphi_1 = 0^\circ$). Among the BW NDI (Table 3), half compounds have the horizontal alkyl chains, while the others have the vertical chains.

The total intermolecular potential increases in proportion to the alkyl chain length, n (Fig. S6(a)). The vertical intercept corresponds to the potential of the core part, and the slope comes from the alkyl part. The slope is the same for different core parts, indicating that the alkyl part makes the same contribution. Since the linearity is perfect, the small anomaly indicates some structural difference. C_n PTTP (red) has HB structures in general, but the hump at $n = 3 - 5$ is associated with the stacking structures (Table 2). The actual stacking structure is slightly less stable than the hypothetical HB structures. The humps of C_n PSeSeP (pink) at $n = 10$ and 14 are also due to the stacking structures (Table 2), which are unstable in comparison with the θ -structures at $n = 8$ and 12 (Table 1).

When we investigate the dispersion and static parts independently in C_n PTTP (Fig. S6(b)), the dispersion (vdW from eqn (S6)) parts increase with n , whereas the electrostatic part (eqn (S7)) becomes almost constant at large n (Fig. S6(c)). The electrostatic term of the core part increases with increasing the ring number, m (Fig. S6(d)). The alkyl chain is almost nonpolar, and gives rise to no Coulomb contribution in contrast to the ordinary aromatic cores. From the basic electromagnetism, if one imagines a cylinder with a central negative charge surrounded by a surface positive charge, the total electrostatic attraction is zero as far as the total charge is neutral. This happens even though the negative charge on an alkyl carbon atom surrounded by two or three hydrogen atoms is significantly larger than that of the aromatic carbon atoms with at most one hydrogen atom. It is characteristic that the stacking arrangement in SHB and θ -structures (TTT) lead to positive (repulsive) $V_{s\ stat}$, though the HB compounds have negative (attracting) V_{stat} (Fig. S6(d)).

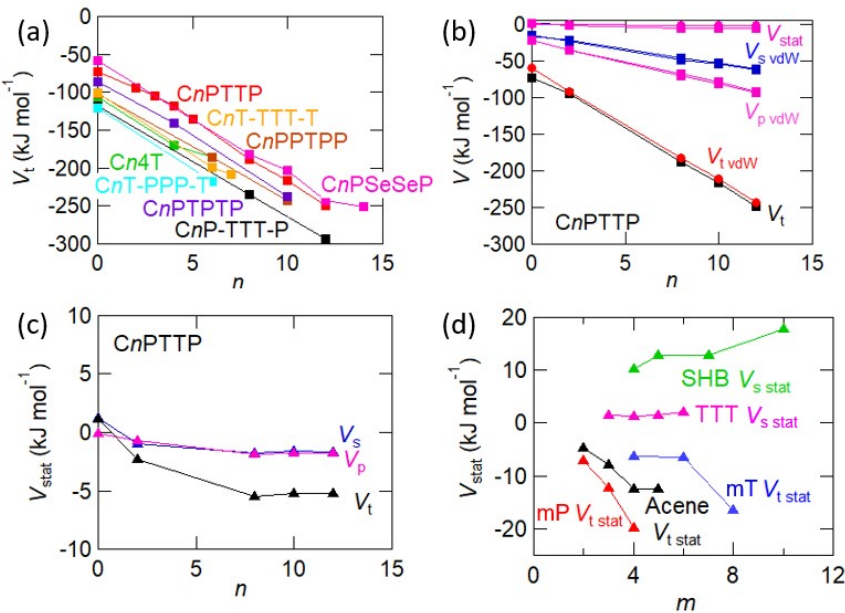
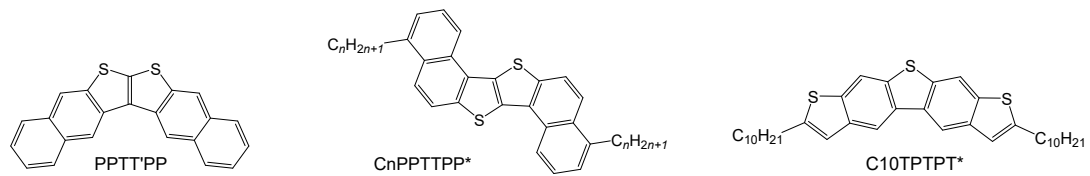


Fig. S6 (a) Total potential of alkylated compounds as a function of the alkyl chain length, n . (b) Dispersion (vdW), static, and total contributions in C_n PTTP, and the (c) electrostatic parts. (d) Ring number, m , dependence of the static contribution in various structures.

Table S10 Structure parameters of compounds where the unsubstituted and alkyl compounds have different structures

Compound		θ (°) c	X_g (Å) ^a	Y_g (Å) ^a	Z_g (Å) ^a	V_g (kJ mol ⁻¹)	X_s (Å)	Y_s (Å)	Z_s (Å)	V_s (kJ mol ⁻¹)	ϕ_1/ϕ_2 (°)	b	CCDC
PSeSeP	HB	62.7	0.38	-0.41	5.15	-27.21	0.38	5.13	3.13	-20.18			607975
C8PSeSeP	θ	113.5	0.50	3.51	4.81	-41.35	0.02	2.30	3.50	-99.26	32/22	h	730254
C12PSeSeP	θ	105.5	0.06	2.95	4.97	-62.00	0.39	2.64	3.50	-118.75	22/23	h	730256
C10PSeSeP	Ila		0.21	4.72	3.03	-53.10	5.78	2.58	3.63	-101.34	23/2	h	730255
C14PSeSeP	Ila		0.51	4.61	3.08	-63.69	6.12	1.76	3.64	-121.93	14/2	h	730257
PTPTP	HB	56.5	5.52	-0.72	4.64	-26.96	0.13	5.20	2.79	-26.29			667690
PTPTP	θ	125.2	5.19	4.04	4.32	-16.50	0.00	1.81	3.50	-53.92			668464
C4PTPTP	Ib		6.88	6.12	2.34	-28.14	3.04	0.02	3.43	-84.37	12/39	v	667691
C10PTPTP	θ	109.1	0.16	3.15	4.89	-60.63	0.07	2.49	3.50	-116.12	26/13	h	1964819
C10PTPTP-P	HB	51.0	0.22	-1.10	4.81	-75.22	0.36	5.53	2.63	-46.89	24/19	v	2312364
PPTPTPP	θ	126.6	8.21	4.02	4.32	-20.53	0.04	1.77	3.52	-78.74			980613
C10PPTPTPP	HB	46.2	0.18	-1.30	4.75	-106.57	0.41	5.62	2.40	-68.53	26/13	v	980612
PTTTP	HB	56.5	0.00	-0.62	4.83	-34.35	0.00	5.20	2.79	-23.19			600120
C6PTTPP	θ	118.4	0.00	3.65	4.71	-41.08	0.00	2.11	3.54	-90.02	28/19	h	830987
T-TTT-T	θ	133.4	0.00	4.39	3.80	-20.28	0.00	1.57	3.64	-60.77			258755
C6T-TTT-T ^c	HB	57.8	2.20	-0.49	4.80	-75.83	0.20	4.95	2.73	-47.95	14/0	v	655866
C7T-TTT-T ^c	HB	58.8	1.25	-0.50	4.69	-77.68	0.09	4.80	2.71	-53.57	18/0	v	969085
PPTT'PP A	γ	74.7	0.69	2.37	6.90	-23.02	4.22	1.91	3.45	-56.62			1523533
		72.3	1.30	0.99	7.19	-25.47	4.06	2.29	3.40	-55.70			
PPTT'PP B	γ	129.3	1.64	6.70	5.35	-6.18	0.10	1.65	3.49	-67.03			1523534
C4PPTTPP*	Ib		3.33	6.76	2.53	-34.61	3.21	0.86	3.49	-94.64	1/31	v	1995852
C6PPTTPP*	Ib		0.64	6.62	2.79	-30.47	7.76	0.61	3.50	-90.98	11/1	h	1995853
C8PPTTPP*	Ib		5.48	6.65	2.90	-35.23	5.48	0.98	3.49	-114.73	7/6	h	1995854
C10PPTTPP*	Ib		3.28	6.30	3.21	-38.05	10.42	0.94	3.55	-112.41	4/1	h	1995855
TPTPT	Ila		0.00	5.41	2.78	-21.95	0.00	1.78	3.46	-52.59			254385
C10TPTPT*	HB	34.1	0.43	-4.30	4.94	-50.18	0.27	5.69	2.19	-46.95	20/34	o	1503965
TTPTT	III	105.8	3.12	6.19	2.71	-9.90	2.62	0.20	3.48	-53.49			1434834
C6TTPTT	Ib		0.44	5.98	2.24	-39.38	3.80	0.86	3.86	-82.15	41/15	h	717515

^a X_{sl} , Y_{sl} , and Z_{sl} for stack (IIa, Ib, and III) structures. ^b h: horizontal, v: vertical, and o: oblique alkyl chains. ^c Alternate HB and stacking patterns.



Alkyl groups in $C_nPSeSeP$ ($n = 8 - 14$) extend in the horizontal direction in the θ-structures and in the direction parallel to the molecular plane ($\phi_2 = 2^\circ$) in the BW (Ila) structures (Table S10).

PTPTP is characterized by the large $X_g > 5 \text{ \AA}$ both in the HB and θ-structures, where the half molecule forms the T-type arrangement excluding the thiophene part (Fig. S7(a)). This anomaly is

entirely removed in C10PTPTP; this compound forms an ordinary θ -structure with nearly zero X_g and X_s . In C4PTPTP, the comparatively large X_s ($\sim 3 \text{ \AA}$) is a standard value among the stacking (Ib) compounds (Table 2). The alkyl chain of this compound extends vertical to the molecular plane ($\phi_l = 12^\circ$), which is typical of the stacking (Ib) structures (Table 2). The HB structure of C10PTPTP-P is formed due to the phenyl substitution; a conjugated phenyl ring with four side hydrogens induces the HB structure more strongly than a fused phenyl ring with only two side hydrogens. Similarly to PTPTP (Fig. S7(a)), PPTPTPP is characterized by the large $X_g > 8 \text{ \AA}$, but C10PPTPTPP forms an ordinary HB structure with $X_g = 0.18 \text{ \AA}$. In general, compounds with a PTPTP unit (PTPTP and PPTPTPP) are characterized by a θ -structure with a large X_g , but the alkyl derivatives have the ordinary HB (sometimes θ -) structures with a small X_g ; this is an origin of the unusual transformation from θ to HB.

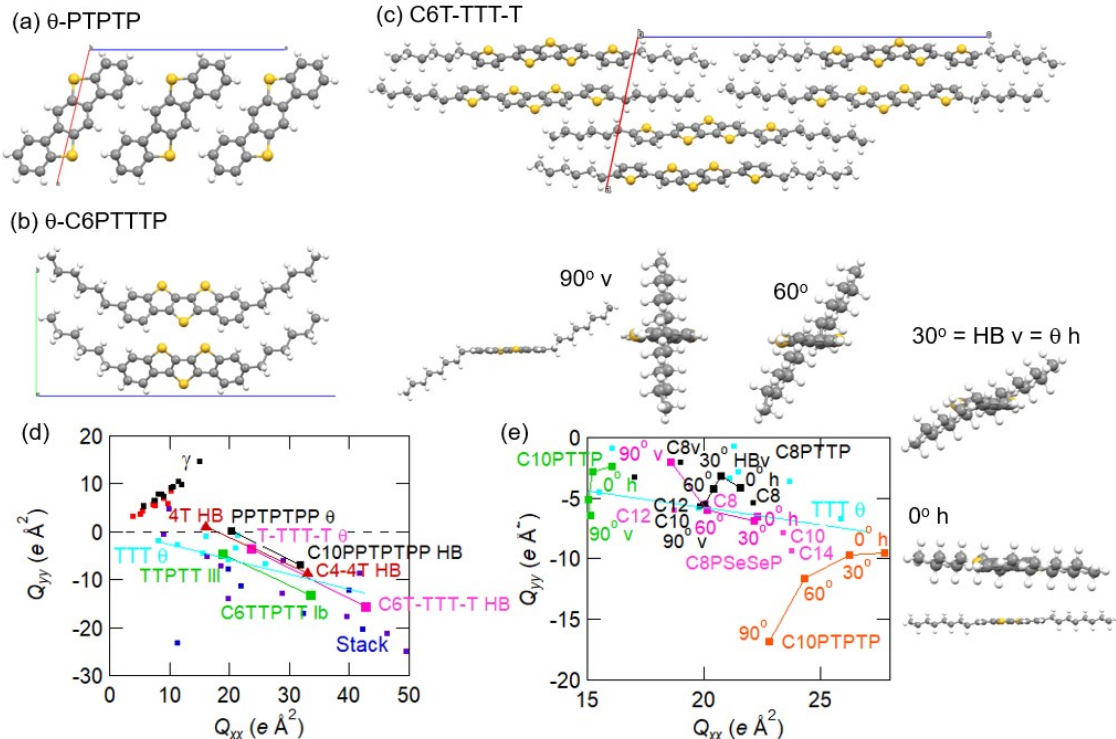


Fig. S7 Crystal structures of (a) θ -PTPTP, (b) θ -C6PTTP, and (c) C6T-TTT-T. (d) Influence of alkylation in the $Q_{xx}Q_{yy}$ -phase diagram. (e) Alkyl orientation dependence of Q_{xx} and Q_{yy} in C8PTTP, C10PTTP, C8PSeSeP, and C10PTPTP.

In C6PTTP and C_nT -TTT-T ($n = 6$ and 7), the alkyl chains are tilted into the same side owing to the odd number of fused thiophenes (Fig. S7(b)). In C_nT -TTT-T ($n = 6$ and 7), the alkyl chains are interpenetrated to every two HB columns (Fig. S7(c)), and this is the origin of the θ to HB transformation. In these cases (PPTPTPP and T-TTT-T), the right down movement in the $Q_{xx}Q_{yy}$ -

phase diagram is the same as PTTP (Fig. S7(d)).

Alkyl orientation dependence of Q_{xx} and Q_{yy} is depicted in Fig. S7(e). In general, the 0° orientation has the largest Q_{xx} .

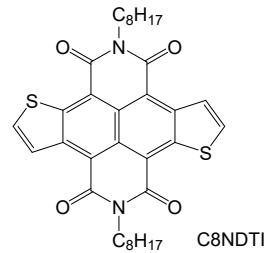
Although PPTPP is HB,¹³ PPTT'PP (Table S10) is no more HB. PPTTPP* has a different fused manner, and the alkyl forms have stacking (Ib) structures. The alkyl chain of C10TPTPT* is not parallel to the crystallographic axes, but since the molecule does not have an inversion center, the alkyl chains are parallel to each other within a layer. The unsubstituted analogue has a stacking (IIa) structure.

Stacking structures of NDI and PDI compounds

Table S11 Supplementary structure parameters of NDI and PDI compounds

Compound	<i>a</i> (Å)	<i>b</i> (Å)	<i>X_s</i> (Å)	<i>Y_s</i> (Å)	<i>Z_s</i> (Å)	<i>V_s</i> (kJ mol ⁻¹)
0						<i>V_g</i>
PDI	14.678/2	4.879	10.91	3.36	3.12	-18.63
C1PDI	14.597	3.874	10.07	5.93	0.01	-9.81
Stack Ia (brickwork)						<i>V_s</i>
NDI	7.6356	8.2211/2	3.63	9.29	0.48	-5.24
C2NDI	4.8667	4.8667	4.66	7.88	0.17	-7.99
C4NDI	7.840	5.223	4.50	7.94	0.13	-11.10
C5NDI	8.1071	5.0282	5.39	7.87	0.11	-18.36
C6NDI	8.284	4.898	5.16	7.80	0.25	-19.64
C7*NDI	8.4203	6.8695	1.97	8.11	1.09	-7.69
C8NDI	6.5335	4.7814	4.29	7.91	0.08	-11.43
C10NDI	6.5503	4.7502	4.07	8.02	0.07	-14.20
C12NDI	6.5900	4.6101	4.21	7.89	0.02	-14.80
C14NDI	6.637	4.637	4.19	7.95	0.03	-16.41
CH ₃ SC3NDI	8.0500	4.9407	5.27	7.83	0.14	-14.63
C4OPNDI	8.1371	4.1636	5.52	6.69	1.86	-28.03
P-PDI	7.5227	5.1360	4.51	7.91	0.22	-11.29
FPC2NDI	7.8416	4.8947	4.84	7.88	0.09	-17.45
DCF ₃ PC1NDI	11.655	4.7402	6.73	4.26	8.51	-11.99
Cy5NDI	6.0407	5.2404	4.01	7.99	0.17	-10.08
Cy6NDI	8.541	6.678	1.63	8.38	0.00	-2.72
Cy7NDI	6.211	5.236	3.84	7.95	0.47	-12.94
Cy8NDI	8.96	7.095	3.67	8.08	1.24	-13.96
C8PDI	6.6707	4.7101	4.15	8.12	0.08	-12.18
PC2PDI#	7.7048	5.0225	5.93	8.14	0.02	-11.58
PCH3C2PDI	9.1410	4.9820	5.93	8.14	0.01	-11.58
fPC2PDI			4.59	8.15	0.11	-20.29
Cy6PPPDI ^a		5.2092	6.33	6.19	1.70	-32.21
g	$\theta = 72.8$	0.03	0.46	5.01	-50.48	
Cy6PZPDI	6.1694	5.1483	2.79	6.89	0.55	-18.28
Stack Ib						
C3NDI	17.24/2	6.9622	3.77	8.19	1.05	-10.43
C4PDI	9.396	4.734	8.86	7.96	0.69	-14.02
C5PDI	8.479	4.754	9.07	7.85	0.77	-13.72
C2OC2PDI	8.306	4.835	8.68	7.83	0.74	-13.73
C1OC3PDI	9.418	4.725	8.87	7.69	0.94	-22.18
C2OC3PDI	8.657	4.747	8.89	7.81	0.52	-13.17
CH ₃ OPC1PDI	9.709	4.390	8.71	7.74	1.17	-14.81
C ₄ F ₇ PDI	8.4835	4.9104	9.07	7.88	0.83	-12.20
PC2PDI		4.7410	9.85	7.24	1.60	-24.35
Stack IIb (pitched π -stack)						<i>V_g</i>
C4PDI	9.396	4.734	8.86	7.96	0.69	-14.02
C5*PDI	8.789	8.157	8.86	7.84	0.67	-19.80
Stack III						<i>V_s</i>
PC1PDI	16.78/2	4.7460	15.57	5.61	5.51	-15.76

^a Alternate BW and γ patterns.



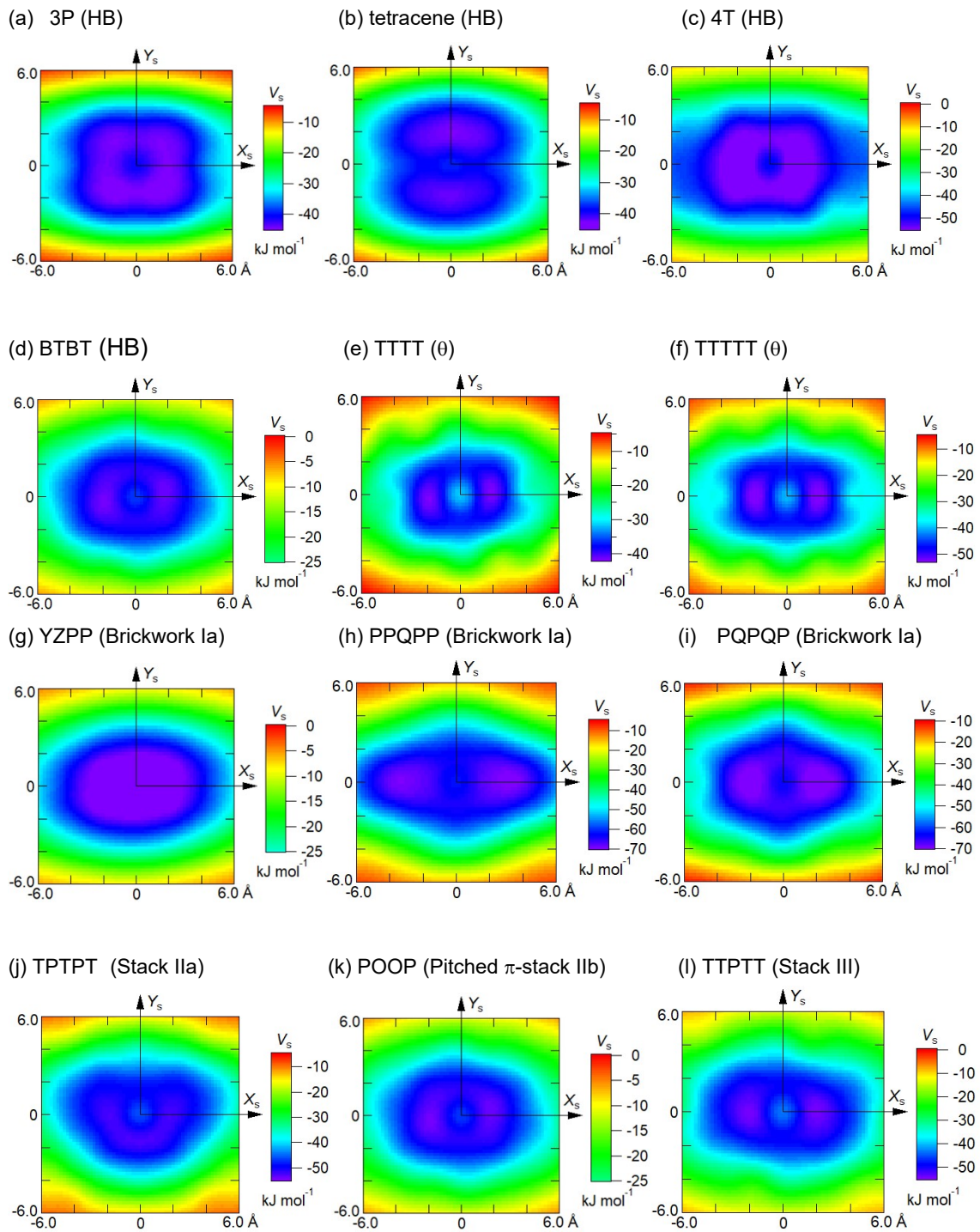


Fig. S8 $X_s Y_s$ -maps of various molecules.

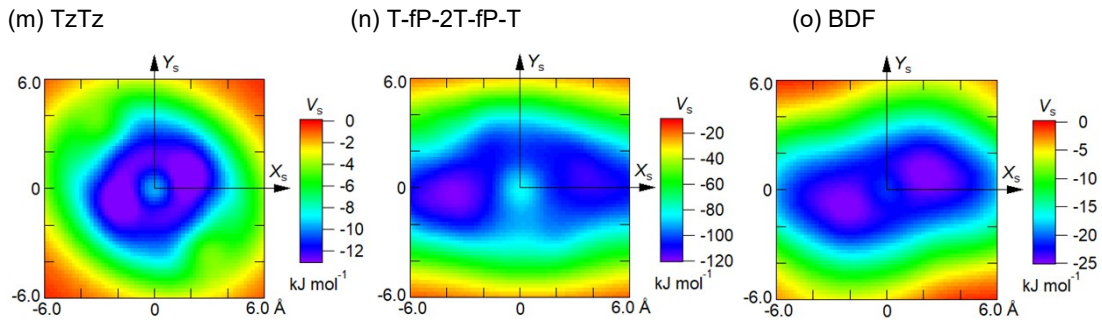


Fig. S8 (continued) X_sY_s -maps of various molecules.

Minima of the X_sY_s -maps indicate that the X_s offset is preferred in general. Exceptions are nP and acenes (Fig. S8(a) and (b)), which show the Y_s offset. The Y_s offset appears in polar molecules, where the electrostatic repulsion at the stacking structure is large. Even PPQPP and PQPQP show the X_s offset (Fig. S8(h) and (i)), and the X_sY_s -maps are not very useful to predict the crystal structure. However, the Y_s offset is a token of polar molecules, and if the HB packing is not possible, the brickwork structure is most likely.

Compounds with blocking groups

Table S12 Structure parameters of compounds with blocking groups.

Compound ^a	μ_{\max} (cm ² V ⁻¹ s ⁻¹) ^c	θ (°)	W (Å)	X_g (Å)	Y_g (Å)	Z_g (Å)	V_g (kJ mol ⁻¹)	X_s (Å)	Y_s (Å)	Z_s (Å)	V_s (kJ mol ⁻¹)	CCDC	Ref
HB													
C1-4T		62.6	4.77	1.14	-0.32	4.72	-40.63	2.35	4.65	2.85	-35.83	1262525	S88
α -2CH ₃ T-TPT	0.023	63.6	4.87	3.89	-0.06	4.87	-28.43	0.30	4.80	2.98	-26.41	1558838	S89
α -2CH ₃ T-TPT ^{a,b}		58.0	4.72	0.08	-0.67	4.72	-33.57	1.12	5.02	2.74	-24.81	1558839	S89
			4.73	0.09	-0.68	4.74	-35.24	0.86	5.03	2.80	-25.36		
θ													
β -2CH ₃ Se-TPT		156.7	8.86	0.23	6.58	3.11	-11.55	4.20	0.81	3.49	-40.39	2125887	10
β -2CH ₃ Se-SePSe		156.4	8.26	0.08	6.65	3.15	-13.48	4.15	0.53	3.51	-55.86	1955298	S90
2CH ₃ T-PPP ^d	0.25	148.0	9.28	0.24	6.63	3.70	-13.01	4.04	0.36	3.45	-44.69	2255048	S91
4CH ₃ Se-pyrene		133.8	6.54	9.76	6.06	4.88	-18.40	3.86	1.81	3.54	-86.19	2302653	S92
0-P π													
β -2CH ₃ O-TPT	0.19	136.3	7.89	0.66	4.45	4.04	-12.22	4.57	2.50	3.39	-35.01	2125884	10
β -2CH ₃ O-SePSe	0.54	146.7	5.18	1.36	6.05	3.62	-9.61	4.89	0.20	3.50	-36.14	2125890	10
β -2CH ₃ T-SePSe	1.7	135.4	8.13	4.16	4.13	4.18	-16.67	4.58	3.02	3.49	-41.42	2125891	10
β -2CH ₃ Se-SePSe	1.6	130.0	8.19	4.14	3.77	4.44	-20.57	4.49	3.31	3.53	-47.09	2125892	10
2CH ₃ T-PPP ^d	0.25	137.7	9.24	0.01	6.17	4.24	-13.14	4.10	0.04	3.43	-43.94	2255047	S91
Stack Ia (BW)													
4(CH ₃ T)		7.12	2.64	2.79	3.61	-63.33	0.23	4.66	3.44	-41.65	1288627	S92	
Stack Ib (long-axis BW)													
TIPS-pentacene ^e	1		6.69	0.93	3.40	-84.16	9.51	1.71	3.32	-44.21	172476	S93	
TMS-pentacene ^e	0.1		4.57	1.16	3.44	-81.10	9.42	5.76	2.18	-21.95	178599	S94	
β -2CH ₃ Se-TPT	0.96	7.76	3.98	0.56	3.48	-47.37	8.08	2.45	3.51	-19.58	1955295	S90	
4CH ₃ O-pyrene	0.03	6.79	5.69	0.33	3.54	-49.22	7.37	0.47	3.61	-39.42	2302650	S95	
4CH ₃ T-pyrene	32	6.55	5.51	0.14	3.55	-63.21	8.74	0.30	3.75	-33.05	2076082	9	
4CH ₃ Se-pyrene	7.3	6.54	5.56	0.33	3.55	-74.67	8.82	2.02	3.72	-40.87	2302656	S95	
4CH ₃ T-perylene I	0.2	8.96	3.38	1.03	3.39	-88.37	9.45	2.72	3.65	-29.71	2269571	S96	
4CH ₃ T-perylene II		8.97	3.37	0.84	3.40	-89.66	9.43	2.80	3.60	-29.46	2269574	S96	
4CH ₃ T-dibenzoperylene		6.53	5.75	0.04	3.46	-97.05	12.77	0.46	3.81	-35.37	2256599	S97	
Stack IIb (P π)			7.17										
Rubrene	40	62.3		6.16	0.00	3.72	-58.18	6.81	0.00	4.32	-41.99 ^g	605654	S98
β -2CH ₃ T-TPT	2.1	89.4	8.53	3.93	0.74	3.53	-43.53	1.42	8.16	1.22	-11.38	1558840	10, S89
β -2CH ₃ Se-TPT	0.26	87.6	7.17	4.00	0.37	3.51	-47.83	2.85	8.05	1.27	-11.80	2125888	10
β -2CH ₃ Se-SePSe	0.45	88.4	7.23	3.97	0.27	3.54	-56.37	2.67	8.10	1.20	-16.67	1955297	S90
2CH ₃ T-PPPP ^f	0.84	86.4	9.23	3.83	0.83	3.45	-60.59	0.31	7.52	2.15	-14.75	2255050	S91
4CH ₃ T-PPPP ^g	0.94	80.9	9.36	3.93	0.10	3.35	-76.40	2.15	9.41	2.81	-13.27	2255051	S91
β -2CH ₃ T-TPPT	0.35	89.2	7.88	3.93	0.48	3.49	-56.73	4.72	7.88	1.81	-14.14	1899661	S99
β -2CH ₃ T-TPPPT	4.08	68.8	7.69	5.79	0.49	3.47	-58.94	6.34	7.73	1.76	-16.93	1899662	S99
β -2CH ₃ Se-TTTT		83.4	8.91	5.09	0.57	3.57	-44.59	4.42	5.17	2.30	-12.88	2068982	S100
Stack III													
6T		83.3	5.37	3.78	1.23	3.54	-93.96	2.52	5.78	3.31	-16.45	164573	S92
β -2CH ₃ O-TPT		79.6	7.89	4.17	0.79	3.53	-36.61	1.61	7.01	0.86	-8.66	2125885	10
β -2CH ₃ O-SePSe		79.0	8.09	4.25	0.86	3.58	-42.18	2.73	6.34	2.70	-10.51	2125889	10
β -2CH ₃ T-SePSe	0.23	84.48	8.22	3.86	0.58	3.55	-47.73	1.53	7.45	3.47	-6.73	1955296	S90

^a Two crystallographically independent molecules. ^b Another polymorph. ^c Field-effect hole mobility. ^d 1,5-Bis(methylthio)anthracene has 0 and 0-P π polymorphs. ^e TIPS: triisopropylsilyl ethynyl, TMS: trimethylsilyl ethynyl. ^f 1,7-Bis(methylthio)tetracene. ^g 1,4,7,10-Tetrakis(methylthio)tetracene.

Compounds with blocking groups are listed in Table S12. For example, 4T with terminal methyl groups (C1-4T) has a HB structure, but an oligomer of β -methyl thiophene, 4(CH₃T), has a BW (stack Ia) structure owing to the blocking effect of the methyl groups at the molecular side. Many β -alkylated oligothiophenes have been investigated for modelling poly(alkylthiophene),^{S101-S106} which have usually stack (most frequently Ia) structures.

TIPS-pentacene (TIPS: triisopropylsilyl ethynyl) has a stacking (Ib) structure but characterized by the large X_{s1} and X_{s2} (Table S12).⁷ In this long-axis BW structure, the interlayer interaction (V_c) is the

second largest interaction (Table S12), and amounts to more than half of V_{s1} . However, the methyl analogue (TMS-pentacene) has a much one-dimensional structure with isolated stacks having small V_{s2} . The long-axis BW structure achieves two-dimensional structures and high-performance transistor materials, but the magnitude of the second interaction is susceptible to the substituents similarly to the NDI derivatives.

Rubrene is an important transistor material,^{S107,S108} where the tetracene part has a P π structure with large V_g (Fig. 12(f)),^{S109} while the phenyl part forms a SHB-like structure. It is characteristic that non-parallel V_g is not significantly smaller than V_{s1} . This is because $X_{s1} = 6.16 \text{ \AA}$ amounts to half of the molecular length (11.43 \AA).

The molecular width of β -2CH₃T-TPT ($> 8 \text{ \AA}$) is much larger than 4.7 \AA of TPT and α -2CH₃T-TPT.¹³ These compounds sometimes form the θ -structure (Table S12), but the θ values are larger ($> 130^\circ$ and sometimes $> 150^\circ$) than the ordinary θ -phase ($125 - 130^\circ$); these compounds are regarded as intermediate between the θ - and the stacking structures.

In the methoxy (CH₃O-), methylseleno (CH₃Se-), and SePSe derivatives, various structures appear depending on whether the intralayer (intercolumnar) and interlayer arrangements are parallel or not (Fig. S9(a)). In addition, there are a considerable number of polymorphs (Table S14). The stacking geometry (V_s) is, however, not largely different (Table S12), where the overlap mode depicted in Fig. S9(b) is the typical one. Z_s in the θ -structure and Z_{s1} in the stacking (Ib, IIb, and III) structures are the interplanar spacing (3.5 \AA), Y_s (and Y_{s1}) is small ($< 1 \text{ \AA}$), and X_s is about 4 \AA (Table S12). The tilt angle of the molecules in the stack is obtained by $\tan \delta = X_s/Z_s$. For example, this value is as large as 48° in β -2CH₃T-TPT, because the large X_s (3.93 \AA) leads to large δ . OPO does not take this structure; although the unsubstituted OPO is HB (Table S5), β -2CH₃X-OPO has dimer structures (Table S15).

4CH₃T-pyrene and perylene (Fig. 12(j) and S9(g)) form the long-axis BW structure similar to TIPS-pentacene characterized by small $Y_{s1} < 1 \text{ \AA}$ (Fig. 12(f)). The interlayer interaction V_c is the second largest interaction (Table S12), and amounts to half of V_{s1} . The difference between X_{s1} and X_c corresponds to the unbalance from the ideal BW structure. In particular, 4CH₃T-pyrene exhibits high-performance in the single-crystal transistors,^{9,11} where V_c is more than half of V_{s1} . The molecular width of 4CH₃T-pyrene (6.55 \AA) is not larger than 6.77 \AA of pyrene, whereas 8.9 \AA of 4CH₃T-perylene is larger than 8.42 \AA of perylene; this is obvious from the molecular structures.

By contrast, methylthio-substituted tetracene (PPPP), TPPT, and the related compounds have a P π (IIb) structure (Fig. S9(d)) again with small $Y_{s1} < 1 \text{ \AA}$. The side interaction V_{s2} with large Y_{s2} (Table S13) is comparable to the interlayer V_c with large X_c (Table S12). However, these values are considerably smaller than V_{s1} . In the $Q_{xx}Q_{yy}$ -diagram, β -2CH₃T-TPT, 4CH₃T-pyrene, 4CH₃T-perylene, 4CH₃T-PPPP, and β -2CH₃T-TPPPT are located in the stacking Region (8) in Fig. 4(b), but β -2CH₃T-TPPT is found in Region (4) in Fig. 5(a); all are in agreement with the stacking or P π structure.

In the ordinary $P\pi$ structures, all molecules are parallel in the layer, but the intralayer tilted version appears frequently (Fig. S9(e)). These structures are categorized as θ - $P\pi$ (Table S12, this structure is simply called $P\pi$ in Ref. 10). The intralayer θ is 130-140° (Table S12), while the interlayer θ is around 80° (Table S13). V_{s2} is again comparable to V_c . The β -substituted SePSe prefers this structure.

Sometimes a long-axis SHB structure appears (Fig. S9(f) and Table S15). The ordinary HB structure has non-parallel contacts along the molecular long side, and the twisted dimer version is the SHB structure. Contrarily, the $P\pi$ has non-parallel contacts at the molecular terminal, and the twisted dimer version is the long-axis SHB. A similar structure is universally observed in the neutral crystal of bis(ethylenedithio)tetrathiafulvalene (BEDT-TTF) and the related compounds, whose charge-transfer salts have been extensively studied as organic superconductors.^{S11}

It is noteworthy that these methylthio compounds do not make BW structures. This is probably because the BW structure is formed in polar molecules. The dimer and long-axis SHB phases do not show transistor properties; transistor properties are observed in the θ - and stacking (Ib and IIb) phases. In the long-axis SHB structures, Z_{s1} is the interplanar spacing (about 3.5 Å). When X_{s1} is not small (> 1 Å), θ is smaller than 80°.

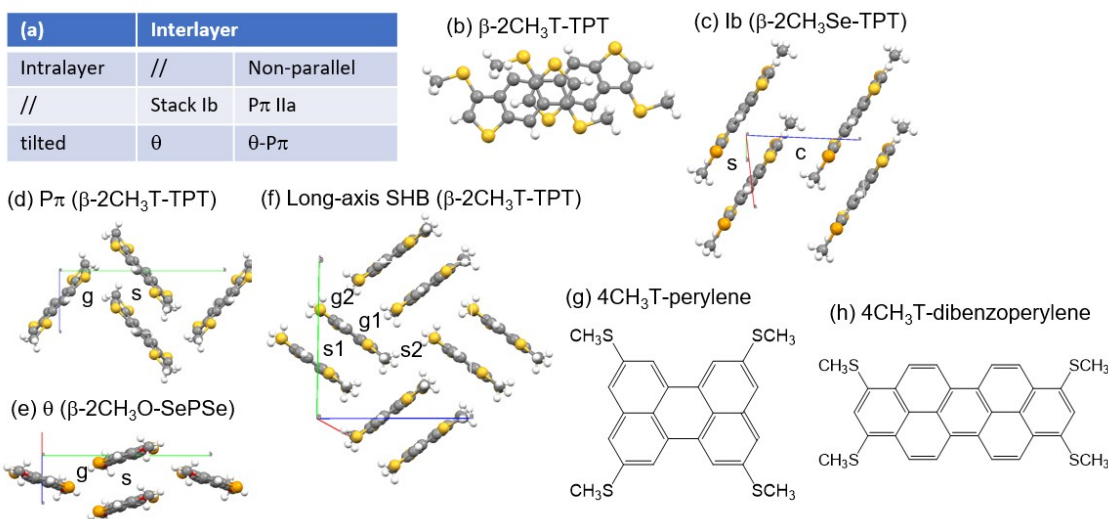


Figure S9 (a) Classification of intra/interlayer parallel/tilted structures. (b) Representative overlap mode in a β -2CH₃T-TPT stack. Crystal structures of (c) stack Ib (β -2CH₃Se-TPT), (d) $P\pi$ (β -2CH₃T-TPT), (e) θ - (β -2CH₃O-SePSe, viewed from the molecular long axis), and (f) long-axis SHB structures (β -2CH₃T-TPT). Molecular structures of (g) 4CH₃T-perylene, and (h) 4CH₃T-dibenzoperylene.

Table S13 Supplementary structure parameters of compounds with blocking groups

Compound	<i>b</i> (Å)	θ (°)	<i>X</i> (Å)	<i>Y</i> (Å)	<i>Z</i> (Å)	<i>V</i> (kJ mol ⁻¹)	CCDC
θ							
β -2CH ₃ Se-TPT	5.5213	156.7	10.02	4.18	1.84	-8.66	2125887
β -2CH ₃ Se-SePSe	8.4327/2	156.4	7.89	3.24	3.55	-25.84	1955298
2CH ₃ T-PPP	5.3222	148.0	7.43	3.68	3.53	-23.35	2255048
4CH ₃ Se-pyrene	5.5408	133.8	10.65	0.77	3.72	-25.57	2302653
θ -P π							
β -2CH ₃ O-TPT	6.2140	80.5	6.58	0.05	3.73	-12.63	2125884
β -2CH ₃ O-SePSe	6.02	80.8	6.47	2.28	3.75	-12.03	2125890
β -2CH ₃ T-SePSe	6.5011	82.1	7.11	0.68	3.86	-17.06	2125891
β -2CH ₃ Se-SePSe	6.5999	85.9	7.40	0.67	3.88	-17.70	2125892
2CH ₃ T-PPP	5.3433	79.9	6.83	3.88	3.95	-15.82	2255047
Stack Ia (BW)							
4(CH ₃ T)	5.274		2.40	7.45	0.17	-20.51	1288627
Stack Ib (long-axis BW)							
β -CH ₃ Se-TPT	5.3202		1.10	7.14	2.23	-9.45	1955295
4CH ₃ O-pyrene	6.7076		2.28	8.06	1.85	-17.21	2302650
4CH ₃ T-pyrene	6.5536		5.23	8.24	2.12	-15.21	2076082
4CH ₃ Se-pyrene	6.6075		2.10	8.48	2.19	-24.34	2302656
4CH ₃ T-perylene I	4.9002		4.50	10.04	1.52	-16.88	2269571
4CH ₃ T-perylene II	4.8598		7.73	9.23	2.18	-10.27	2269574
4CH ₃ T-dibenzoperylene	6.7064		2.21	8.50	1.76	-24.23	2256599
Stack IIb (P π)							
β -CH ₃ T-TPT	5.3415	89.4	6.68	1.19	3.15	-13.83	1558840
β -CH ₃ Se-TPT	5.3366	87.6	6.49	2.17	3.11	-11.46	2125888
β -CH ₃ Se-SePSe	5.3247	88.4	0.58	2.12	3.20	-16.53	1955297
CH ₃ T-PPPP	5.2161	86.4	8.18	1.16	4.87	-15.64	2255050
4CH ₃ T-PPPP	5.1652	80.9	7.87	1.21	5.22	-22.45	2255051
2CH ₃ T-TPPT	5.2771	89.2	7.75	1.79	4.48	-12.80	1899661
2CH ₃ T-TPPPT	6.7687	68.8	0.08	1.66	4.97	-19.41	1899662
2CH ₃ Se-TTTT	6.2428	83.4	7.92	2.76	4.68	-14.35	2068982
Stack III							
6fT ^a	5.3230	83.3	14.08	0.54	10.86	-10.75	164573
β -2CH ₃ O-TPT	5.5283	81.7	6.75	0.02	3.64	-8.63	2125885
β -2CH ₃ O-SePSe	5.6228	81.0	6.73	0.12	3.62	-12.83	2125889
β -2CH ₃ T-SePSe	5.2744	89.7	6.86	1.09	3.37	-12.07	1955296
Long-axis SHB							
β -2CH ₃ O-OPO	7.4386	76.6	2.23	6.99	1.24	-11.91	2125881
β -2CH ₃ T-TPT	7.7368	73.4	1.56	7.23	2.25	-14.43	2125886
			1.41	5.14	4.06	-14.91	
4CH ₃ T-PPP	10.3415	92.1	3.96	9.82	0.63	-9.10	2255049
CH ₃ O-TTTT	11.4018	132.1	1.27	4.77	4.15	-12.27	2068980
		132.1	1.48	4.29	4.25	-15.95	

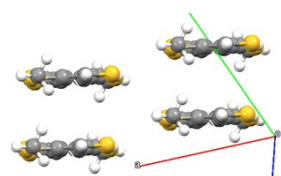
^a P π direction.

Table S14 Polymorphs of $\beta\text{-CH}_3\text{X-TPT}$

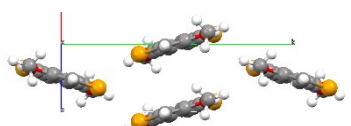
	CH ₃ O-	CH ₃ T-	CH ₃ Se-
OPO	Long axis SHB (2125881)	dimer (2125882)	dimer (2125883)
TPT	$\theta\text{-P}\pi$ (2125884) III (2125885)	$\text{P}\pi$ (1558840) Long axis SHB (2125886)	$\theta//$ (2125887) $\text{P}\pi$ (2125888) Ib (1955295)
SePSe	$\theta\text{-P}\pi$ (2125890) III (2125889)	$\theta\text{-P}\pi$ (2125891) III (1955296)	$\theta//$ (1955298) $\theta\text{-P}\pi$ (2125892) $\text{P}\pi$ (1955297)
TTTT	Long axis SHB θ (2068980)	Long axis SHB (2068981)	$\text{P}\pi$ (2068982)
pyrene	Ib (2302650)	Ib (2076082)	$\theta//$ (2302653) Ib (2302656)
PPP		2CH ₃ T- $\theta//$ (2255048) $\theta\text{-P}\pi$ (2255047)	4CH ₃ T- Long axis SHB (2255049)
PPPP		P π (2255050)	P π (2255051)

Structures with the same color are isostructural.

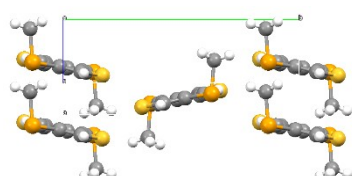
(a) $\text{P}\pi$ (CH₃T-TPT)



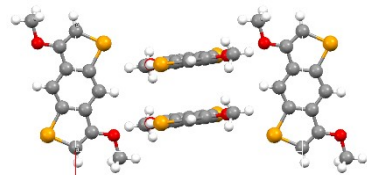
(b) $\theta\text{-P}\pi$ (CH₃O-SePSe)



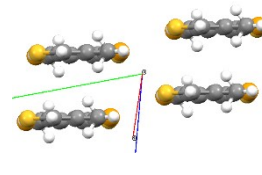
(c) $\theta//$ (CH₃Se-TPT)



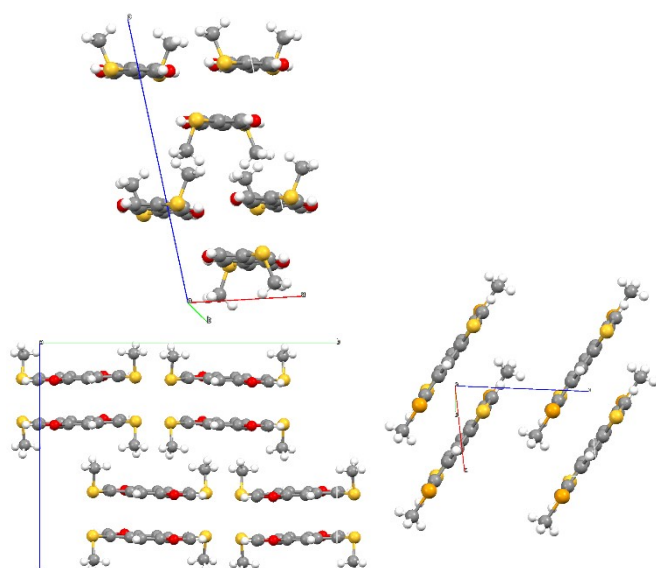
(d) III (CH₃O-SePSe)



(e) Ib (CH₃Se-TPT)



(f) dimer (CH₃T-OPO)



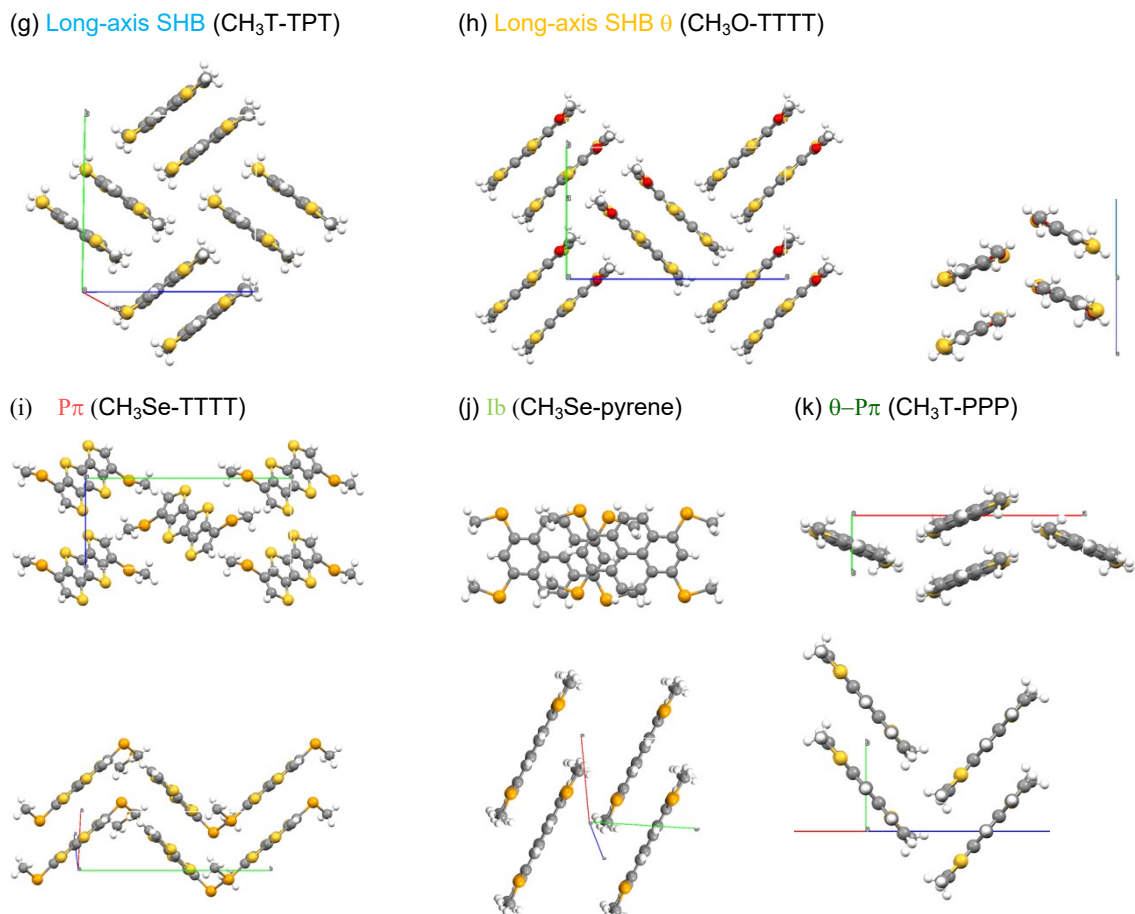


Fig. S10 Crystal structures of CH_3X -TPT, CH_3X -TTTT, CH_3X -pyrene, and CH_3X -PPP.

Table S15 Structure parameters of compounds with long-axis SHB structures

Compound	$\mu_{\max} (\text{cm}^2 \text{V}^{-1} \text{s}^{-1})^{\text{a}}$	$\theta (\text{°})$	$W (\text{\AA})$	$L (\text{\AA})$	$X_g (\text{\AA})$	$Y_g (\text{\AA})$	$Z_g (\text{\AA})$	$V_g (\text{kJ mol}^{-1})$	$X_s (\text{\AA})$	$Y_s (\text{\AA})$	$Z_s (\text{\AA})$	$V_s (\text{kJ mol}^{-1})$	CCDC	Ref	
Long-axis SHB					g1/g2			s1/s2							
β -2CH ₃ O-OPO	76.6	7.10	9.62	0.07	1.69	6.27	-14.68	1.09	1.05	3.38	-33.50	2125881	10		
				2.54	4.43	6.01	-10.50	7.34	1.39	3.59	-16.15				
β -2CH ₃ T-TPT ^b	73.4	7.83	10.09	0.76	1.59	6.48	-18.57	1.39	0.83	3.48	-48.79	2125886	10		
	73.4	7.08	10.45	3.85	3.33	6.55	-19.90	9.74	2.06	3.57	-11.37				
				0.55	1.50	6.53	-17.74	2.53	2.49	3.43	-44.67				
				3.25	0.98	6.47	-21.45	8.98	0.68	3.37	-12.46				
4CH ₃ T-PPP ^c	0.005	87.9	9.27	9.31	0.15	0.11	7.30	-28.14	0.06	1.72	3.58	-74.79	2255049	S91	
					3.42	1.84	7.50	-21.61	7.51	1.75	3.60	-32.17			
β -2CH ₃ O-TTTT ^b		6.44	11.76	0.36	3.60	7.74	-15.93	0.08	1.64	3.59	-42.62	2068980	S100		
		83.9	6.45	11.77	3.55	3.11	8.01	-11.78	8.79	2.55	3.97	-25.93			
					0.34	3.42	7.80	-17.05	0.05	1.82	3.50	-44.68			
					3.59	3.04	8.01	-12.94	8.77	2.54	4.01	-21.08			
β -2CH ₃ T-TTTT ^b	75.2	5.97	13.07	0.69	2.62	6.80	-19.18	1.63	0.62	3.50	-61.00	2068981	S100		
					3.28	2.06	6.83	-24.11	10.04	0.70	3.40	-18.78			
	75.4	4.53	13.65	0.51	3.15	6.57	-18.62	1.91	0.60	3.48	-58.70				
					4.34	1.54	7.55	-14.21	9.81	1.38	3.41	-14.26			

^a Field-effect hole mobility. ^b Two crystallographically independent molecules. ^c 1,4,5,8-Tetrakis(methylthio)anthracene.

Quadrupole-quadrupole interaction

Quadrupole-quadrupole interaction is estimated by placing charges $\rho_i = Q_{xx}/2$ on a unit length $x = \pm 1.0 \text{ \AA}$, and similarly $Q_{yy}/2$ and $Q_{zz}/2$ on $y = \pm 1.0 \text{ \AA}$ and $z = \pm 1.0 \text{ \AA}$, respectively. These six point-charges represent the quadrupole moments. The adjacent quadrupole rotated by 90° is placed on $(y, z) = (0, R)$ for A (yz), and a parallel one on (R, R) for B (yz). The Coulomb energy $\rho_i\rho_j/R^2$ is evaluated from these point-charges.

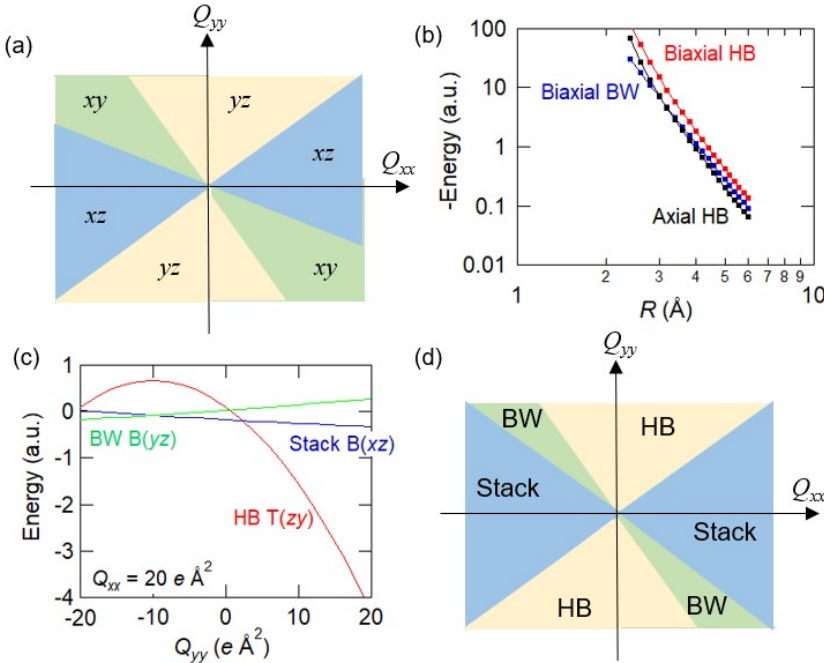


Fig. S11 (a) Regions of the largest A(yz), A(yz), and A(xy) for the same R . (b) R dependence of the quadrupole interaction. (c) Energy of Fig. 13 for $Y_g = Z_0 = 4.80 \text{ \AA}$ along $Q_{xx} = 20 e \text{ \AA}^2$. (d) Largest quadrupole-quadrupole interactions in the $Q_{xx}Q_{yy}$ -diagram at $Y_g = 4.70$ and $Z_0 = 3.45 \text{ \AA}$.

Among the axial interactions, A(xz), A(yz), and A(xy) with the same R , A(yz) is largest (most stable) when Q_{zz} and Q_{yy} are the largest and the second largest moments (absolute magnitudes with opposite signs). This is because that in HB A(yz) in Fig. 13, the closest + and – charges afford the principal contribution, but these charges are $Q_{zz}/2$ and $Q_{yy}/2$. The regions of the largest interactions are shown in Fig. S11(a). B(xz), B(yz), and B(xy) are largest in the same regions. Here, the closest two charge combinations of B(xz) come from $Q_{xx}/2$ and $Q_{zz}/2$ (Stack B(xz) Fig. 13).

The analytical quadrupole energy is proportional to $-Q^2/R^5$.¹¹⁹ The calculated energy also decreases following R^{-5} or steeper (Fig. S11(b)). Accordingly, A(xz), A(xy), and B(xy) are small due to the large $R > L/2$. For example, A(xz) corresponds to an end-on molecular arrangement placed on another molecular plane. The energy of the remaining A(yz), B(xz), and B(yz) are calculated in Fig. S11(c), and the most stable interaction is depicted in Fig. 13. The X_s and Y_s offsets of the actual stacking and BW structures are as small as $1 \sim 4 \text{ \AA}$, but the vertical offsets in B(xz) and B(yz) (Fig. 13) are

assumed to be the same as Z_0 , because this maximizes the biaxial interaction. The maximum of carbon π orbital appears around 0.84 Å. However, only the relative ratio of R is important. Accordingly, $R = Y_g = 4.80$ Å is used in Fig. 13. Actually, $Y_g = 4.70$ Å for the one-leg HB structures in A(yz) should be larger than the typical interplanar distance $Z_0 = 3.45$ Å of B(xz) and B(yz).¹³ In the latter parameters, the HB region is comparatively small (Fig. S11(d)).

References

- S1 A. Gavezzotti, *Acc. Chem. Res.*, 1994, **27**, 309.
- S2 M. Mirsky, *Acta Crystallogr. A*, 1976, **32**, 199.
- S3 D. E. Williams and T. L. Starr, *Computers Chem.*, 1977, **1**, 173.
- S4 S. R. Cox, L.-Y. Hsu and D. E. Williams, *Acta Crystallogr. A*, 1981, **37**, 293.
- S5 D. E. Williams and S. R. Cox, *Acta Crystallogr., Sect. B: Struct. Crystallogr. Cryst. Chem.*, 1984, **40**, 404.
- S6 W. L. Jorgensen and J. Tirado-Rives, *J. Am. Chem. Soc.*, 1988, **110**, 1657.
- S7 J. R. Holden, Z. Du and H. L. Ammon, *J. Comp. Chem.*, 1993, **14**, 422.
- S8 W. D. Cornell, P. Cieplak, C. I. Bayly, I. R. Gould, K. M. Merz, Jr., D. M. Ferguson, D. C. Spellmeyer, T. Fox, J. W. Caldwell and P. A. Kollman, *J. Am. Chem. Soc.*, 1995, **117**, 5179.
- S9 The software is available from <http://indigo1026.la.coocan.jp/lib/exp.html>. (accessed 17 June 2025).
- S10 <https://dasher.wustl.edu/tinker/distribution/params/> (accessed 17 June 2025).
- S11 These compounds are not included in Ref. 13 because the hydrogen coordinates are not given in the original papers. Here, calculated coordinates are used.
- S12 S. Inoue, T. Jigami, H. Nozoe, Y. Aso, F. Ogura and T. Otsubo, *Heterocycles*, 2000, **52**, 159.
- S13 H. Nakanishi, S. Inoue, Y. Aso and T. Otsubo, *Synth. Met.*, 1999, **101**, 639.
- S14 J. Liu, H. Dong, Z. Wang, D. Ji, C. Cheng, H. Geng, H. Zhang, Y. Zhen, L. Jiang, H. Fu, Z. Bo, W. Chen, Z. Shuai and W. Hu, *Chem. Commun.*, 2015, **51**, 11777; J. Liu, H. Zhang, H. Dong, L. Meng, L. Jiang, L. Jiang, Y. Wang, J. Yu, Y. Sun, W. Hu and A. J. Heeger, *Nat. Commun.*, 2015, **6**, 10032.
- S15 D. Zhang, S. Yokomori, R. Kameyama, C. Zhao, A. Ueda, L. Zhang, R. Kumai, Y. Murakami, H. Meng and H. Mori, *ACS Appl. Mater. Interfaces*, 2021, **13**, 989.
- S16 L. Yan, Y. Zhao, H. Yu, Z. Hu, Y. He, A. Li, O. Goto, C. Yan, T. Chen, R. Chen, Y.-L. Loo, D. F. Perepichka, H. Meng and W. Huang, *J. Mater. Chem. C*, 2016, **4**, 3517.
- S17 J. Li, D. Ji, Y. Hu, M. Chen, J. Liu, Z. Qin, Y. Sun, Y. Dang, Y. Zhen, H. Dong, L. Li and W. Hu, *J. Mater. Chem. C*, 2020, **8**, 15597.
- S18 P. F. van Hutten, J. Wildeman, A. Meetsma and G. Hadzioannou, *J. Am. Chem. Soc.*, 1999, **121**, 5910.
- S19 L. Jiang, W. Hu, Z. Wei, W. Xu and H. Meng, *Adv. Mater.*, 2009, **21**, 3649.
- S20 H. Meng, F. Sun, M. B. Goldfinger, F. Gao, D. J. Londono, W. J. Marshal, G. S. Blackman, K. D. Dobbsand and D. E. Keys, *J. Am. Chem. Soc.*, 2006, **128**, 9304.
- S21 L. Zi, J. Zhang, C. Li, Y. Qu, B. Zhen, X. Liu and L. Zhang, *Org. Lett.*, 2020, **22**, 1499.
- S22 K. Takimiya, Y. Kunugi, Y. Toyoshima and T. Otsubo, *J. Am. Chem. Soc.*, 2005, **127**, 3605.
- S23 X. Wu, D. Dai, Y. Ling, S. Chen, C. Huang, S. Feng and W. Huang, *ACS Appl. Mater. Interfaces*, 2020, **12**, 30267.
- S24 H. Meng, F. Sun, M. B. Goldfinger, G. D. Jaycox, Z. Li, W. J. Marshall and G. S. Blackman, *J. Am. Chem. Soc.*, 2005, **127**, 2406.
- S25 M. Suzuki, K. Terai, C. Quinton, H. Hayashi, N. Aratani and H. Yamada, *Chem. Sci.*, 2020, **11**, 1825.
- S26 S. Tavazzi, L. Miozzo, L. Silvestri, S. Mora, P. Spearman, M. Moret, S. Rizzato, D. Braga, A. K. D. Diaw, D. Gningue-Sall, J.-J. Aaron and A. Yassar, *Cryst. Growth Design*, 2010, **10**, 2342.
- S27 A. Y. Sosorev, M. V. Vener, O. G. Kharlanov, E. V. Feldman, O. V. Borshchev, N. I. Sorokina, T. V. Rybalova, S. A. Ponomarenko and D. Y. Paraschuk, *J. Phys. Chem. C*, 2023, **127**, 17948.
- S28 S. Hotta, M. Goto, R. Azumi, M. Inoue, M. Ichikawa and Y. Taniguchi, *Chem. Mater.*, 2004, **16**, 237.
- S29 H. Mizuno, U. Haku, Y. Marutani, A. Ishizumi, H. Yanagi, F. Sasaki and S. Hotta, *Adv. Mater.*, 2012, **24**, 5744.
- S30 R. Jouclas, J. Liu, M. Volpi, L. S. de Moraes, G. Garbay, N. McIntosh, M. Bardini, V. Lemaur, A. Vercouter, C. Gatsios, F. Modesti, N. Turetta, D. Beljonne, J. Cornil, A. R. Kennedy, N. Koch, P. Erk, P. Samori, G. Schweicher and Y. H. Geerts, *Adv. Sci.*, 2022, **9**, 2105674.
- S31 A. Matsunaga, Y. Ogawa, S. Tamura, K. Yamamoto and H. Katagiri, *Chem. Select*, 2021, **6**, 4506.
- S32 Y. Ogawa, K. Yamamoto, C. Miura, S. Tamura, M. Saito, M. Mamada, D. Kumaki, S. Tokito and H. Katagiri, *ACS Appl. Mater. Interfaces*, 2017, **9**, 9902.
- S33 J. Youn, S. Kewalramani, J. D. Emery, Y. Shi, S. Zhang, H.-C. Chang, Y. Liang, C.-M. Yeh, C.-Y. Feng, H. Huang, C. Stern, L.-H. Chen, J.-C. Ho, M.-C. Chen, M. J. Bedzyk, A. Facchetti and T. J.

- Marks, *Adv. Func. Mater.*, 2013, **23**, 3850.
- S34 Y. Lou, R. Shi, L. Yu, T. Jiang, H. Zhang, L. Zhang, Y. Hu, D. Ji, Y. Sun, J. Li, L. Li and W. Hu, *RSC Adv.*, 2023, **13**, 11706.
- S35 I. Wallmann, G. Schnakenburg and A. Lutzen, *Synthesis*, 2009, **79**.
- S36 M. Qi, D. Zhang, Y. Zhu, C. Zhao, A. Li, F. Huang, Y. He and H. Meng, *J. Mater. Chem. C*, 2024, **12**, 6578.
- S37 K. Oniwa, T. Kanagasekaran, T. Jin, M. Akhtaruzzaman, Y. Yamamoto, H. Tamura, I. Hamada, H. Shimotani, N. Asao, S. Ikeda and K. Tanigaki, *J. Mater. Chem. C*, 2013, **1**, 4163.
- S38 O. Gidron, Neta V. Linda, J. W. Shimon and G. L. M. Bendikov, *Chem. Commun.*, 2013, **49**, 6256.
- S39 H. Su, CCDC 604799, Experimental Crystal Structure determination, 2006; M. A. A. Alshajajir, L. J. Higham, P. G. Waddell, CCDC 2405538, *CSD Communication*, 2024.
- S40 J. Iwicki, C. Nather, M. Schiek, A. Lutzen, H.-G. Rubahn, W. Kruger, K. Rossnagel and L. Kipp, *Mater. Lett.*, 2009, **63**, 2399.
- S41 Y. Zhao, L. Yan, I. Murtaza, X. Liang, H. Meng and W. Huang, *Org. Electron.*, 2017, **43**, 105.
- S42 T. Matsuo, C. Rössiger, J. Herr, R. Göttlich, D. Schlettwein, H. Mizuno, F. Sasaki and H. Yanagi, *RSC Adv.*, 2020, **10**, 24057.
- S43 H. Nakai, T. Saito and M. Yamakawa, *Acta Crystallogr. Sect. C: Cryst. Struct. Commun.*, 1988, **44**, 2117.
- S44 W. Yue, H. Tian, N. Hu, Y. Geng and F. Wang, *Cryst. Growth Design*, 2008, **8**, 2352.
- S45 Y. Shibuya, A. Matsunaga, D. Kumaki, S. Tokito and H. Katagiri, *Cryst. Growth Design*, 2022, **22**, 6554.
- S46 S. Ando, D. Kumaki, J. Nishida, H. Tada, Y. Inoue, S. Tokito and Y. Yamashita, *J. Mater. Chem.*, 2007, **17**, 553.
- S47 Y. Yamashita, K. Saito, T. Suzuki, C. Kabuto, T. Mukai and T. Miyashi, *Angew. Chem., Int. Ed.*, 1988, **27**, 434.
- S48 S. Tavazzi, L. Miozzo, L. Silvestri, S. Mora, P. Spearman, M. Moret, S. Rizzato, D. Braga, A. K. D. Diaw, D. Gningue-Sall, J.-J. Aaron and A. Yassar, *Cryst. Growth Design*, 2010, **10**, 2342.
- S49 J. Liu, W. Zhu, K. Zhou, Z. Wang, Y. Zou, Q. Meng, J. Li, Y. Zhen and W. Hu, *J. Mater. Chem. C*, 2016, **4**, 3621.
- S50 L. Chen, Z. Qin, H. Huang, J. Zhang, Z. Yin, X. Yu, X. Zhang, C. Li, G. Zhang, M. Huang, H. Dong, Y. Yi, L. Jiang, H. Fu and D. Zhang, *Adv. Sci.*, 2023, **10**, 2300530.
- S51 S. Ando, J. Nishida, E. Fujiwara, H. Tada, Y. Inoue, S. Tokito and Y. Yamashita, *Chem. Mater.*, 2005, **17**, 1261.
- S52 S. Ando, J. Nishida, H. Tada, Y. Inoue, S. Tokito and Y. Yamashita, *J. Am. Chem. Soc.*, 2005, **127**, 5336.
- S53 T. Kojima, J. Nishida, S. Tokito, H. Tada and Y. Yamashita, *Chem. Commun.*, 2007, 1430.
- S54 T. Kono, D. Kumaki, J. Nishida, T. Sakanoue, M. Kakita, H. Tada, S. Tokito and Y. Yamashita, *Chem. Mater.*, 2007, **19**, 1218.
- S55 J. M. Robertson, H. M. M. Shearer, G. A. Sim and D. G. Watson, *Acta Crystallogr.*, 1962, **15**, 1; B. Dittrich, F. P. A. Fabbiani, J. Henn, M. U. Schmidt, P. Macchi, K. Meindl and M. A. Spackmann, *Acta Crystallogr., Sect. B: Struct. Crystallogr. Cryst. Chem.*, 2018, **74**, 416.
- S56 S. Kashino, M. Haisa, K. Fujimori and K. Yamane, *Acta Crystallogr., Sect. B: Struct. Crystallogr. Cryst. Chem.*, 1982, **38**, 2729.
- S57 Y. Yamaguchi, Y. Maruya, H. Katagiri, K. Nakayama and Y. Ohba, *Org. Lett.*, 2012, **14**, 2316.
- S58 E. G. Cox, R. J. J. H. Gillot and G. A. Jeffrey, *Acta Crystallogr.*, 1949, **2**, 356.
- S59 A. C. Villa, M. Nardelli and C. Palmieri, *Acta Crystallogr. Sect. B: Struct. Crystallogr. Cryst. Chem.*, 1969, **25**, 1374.
- S60 K. Yamamoto, H. Katagiri, H. Tairabune, Y. Yamaguchi, Y. Pu, K. Nakayama and Y. Ohba, *Tetrahedr. Lett.*, 2012, **53**, 1786.
- S61 T. Kimura, Y. Ishikawa, Y. Minoshima and N. Furukawa, *Heterocycles*, 1994, **37**, 541.
- S62 W. Porzio, S. Destri, M. Pasini, A. Rapallo, U. Giovanella, B. Vercelli and M. Campione, *Cryst. Growth Design.*, 2006, **6**, 1497.
- S63 M. Akhtaruzzaman, M. Tomura, J. Nishida and Y. Yamashita, *J. Org. Chem.*, 2004, **69**, 2953.
- S64 S. Ando, R. Murakami, J. Nishida, H. Tada, Y. Inoue, S. Tokito and Y. Yamashita, *J. Am. Chem. Soc.*, 2005, **127**, 5336.

- Soc.*, 2005, **127**, 14996.
 S65 M.-H. Yoon, A. Facchetti, C. E. Stern and T. J. Marks, *J. Am. Chem. Soc.*, 2006, **128**, 5792.
 S66 A. Facchetti, M.-H. Yoon, C. L. Stern, H. E. Katz and T. J. Marks, *Angew. Chem., Int. Ed.*, 2003, **42**, 3900.
 S67 K. Takimiya, K. Kato, Y. Aso, F. Ogura and T. Otsubo, *Bull. Chem. Soc. Jpn.*, 2002, **75**, 1795.
 S68 Y. Ogawa, E. Takiguchi, M. Mamada, D. Kumaki, S. Tokito and H. Katagiri, *Tetrahedr. Lett.*, 2017, **58**, 963.
 S69 I. C. Santos, M. Almeida, J. Morgado, M. T. Duarte and L. Alcacer, *Acta Crystallogr., Sect. C: Cryst. Struct. Commun.*, 1997, **53**, 1640.
 S70 M. Kozaki, S. Tanaka and Y. Yamashita, *J. Org. Chem.*, 1994, **59**, 442.
 S71 S. Langis-Barsetti, T. Maris and J. D. Wuest, *J. Org. Chem.*, 2017, **82**, 5034.
 S72 S. Matsumoto, K. Matsuhama, J. Mizuguchi, *Acta Crystallogr. C: Cryst. Struct. Commun.*, 1999, **55**, 131.
 S73 Y. Dong, H. Li, J. Liu, J. Zhang, X. Shi, Y. Shi, C. Li, Z. Liu, T. Li and L. Jiang, *Org. Electr.*, 2019, **77**, 10537.
 S74 H. von Eller-Pandraud, *Acta Crystallogr.*, 1960, **13**, 936.
 S75 S. Ando, J. Nishida, Y. Inoue, S. Tokito and Y. Yamashita, *J. Mater. Chem.*, 2004, **14**, 1787.
 S76 M. Mamada, J. Nishida, D. Kumaki, S. Tokito and Y. Yamashita, *Chem. Mater.*, 2007, **19**, 5404.
 S77 M. Mamada, J. Nishida, S. Tokito and Y. Yamashita, *Chem. Commun.*, 2009, 2177.
 S78 G. Bolla, J. Guo, H. Zhao, S. Lv, J. Liu, Y. Li, Y. Zhen, Q. Liao, X. Wang, H. Fu, H. Dong, Z. Wang, Z. Wang and W. Hu, *CrystEngComm*, 2022, **24**, 5683.
 S79 D. Xia, X.-Y. Wang, X. Guo, M. Baumgarten, M. Li and K. Müllen, *Cryst. Growth Design*, 2016, **16**, 7124.
 S80 H. R. Yakir, L. J. W. Shimon and O. Gidron, *Helv. Chim. Acta*, 2019, **102**, e1900027.
 S81 E. G. Bryan, A. J. P. White, M. J. D. Attwood and S. E. M. Heutz CCDC 2334205: Experimental Crystal Structure Determination, 2024.
 S82 T. Suzuki, T. Tsuji, T. Okubo, A. Okada, Y. Obana, T. Fukushima, T. Miyashi and Y. Yamashita, *J. Org. Chem.*, 2001, **66**, 8954.
 S83 M. Akhtaruzzaman, N. Kamata, J. Nishida, S. Ando, H. Tada, M. Tomura and Y. Yamashita, *Chem. Commun.*, 2005, 3183.
 S84 Y. Sakamoto, S. Komatsu and T. Suzuki, *J. Am. Chem. Soc.*, 2001, **123**, 4643.
 S85 J. S. de Melo, J. Pina, L. M. Rodrigues and R. S. Becker, *J. Photochem. Photobio. A*, 2008, **194**, 67.
 S86 A. Y. Sosorev, M. V. Vener, O. G. Kharlanov, E. V. Feldman, O. V. Borshchev, N. I. Sorokina, T. V. Rybalova, S. A. Ponomarenko and D. Y. Paraschuk, *J. Phys. Chem. C*, 2023, **127**, 17948.
 S87 X. Wu, D. Dai, Y. Ling, S. Chen, C. Huang, S. Feng and W. Huang, *ACS Appl. Mater. Interfaces*, 2020, **12**, 30267.
 S88 S. Hotta and K. Waragai, *J. Mater. Chem.*, 1991, **1**, 835.
 S89 C. Wang, H. Nakamura, H. Sugino and K. Takimiya, *Chem. Commun.*, 2017, **53**, 9594.
 S90 H. Takenaka, T. Ogaki, C. Wang, K. Kawabata and K. Takimiya, *Chem. Mater.*, 2019, **31**, 6696.
 S91 K. Kanazawa, K. Bulgarevich, K. Kawabata and K. Takimiya, *Cryst. Growth Design*, 2023, **23**, 5941.
 S92 G. Barbarella, M. Zambianchi, A. Bongini and L. Antolini, *Adv. Mater.*, 1992, **4**, 28.
 S93 J. E. Anthony, D. L. Eaton and S. R. Parkin, *Org. Lett.*, 2002, **4**, 15.
 S94 J. E. Anthony, J. S. Brooks, D. L. Eaton and S. R. Parkin, *J. Am. Chem. Soc.*, 2001, **123**, 9482.
 S95 K. Bulgarevich, S. Horiuchi and K. Takimiya, *Chem. Mater.*, 2022, **34**, 6606.
 S96 K. Takimiya, K. Bulgarevich and S. Horiuchi, *J. Mater. Chem. C*, 2023, **11**, 10809.
 S97 K. Bulgarevich, S. Horiuchi and K. Takimiya, *Adv. Mater.*, 2023, **35**, 2305548.
 S98 O. D. Jurchescu, A. Meetsma and T. T. M. Palstra, *Acta Crystallogr. Sect. B: Struct. Crystallogr. Cryst. Chem.*, 2006, **62**, 330.
 S99 C. Wang, D. Hashizume, M. Nakano, T. Ogaki, H. Takenaka, K. Kawabata and K. Takimiya, *Chem. Sci.*, 2020, **11**, 1573.
 S100 K. Takimiya, K. Kanazawa and K. Kawabata, *Cryst. Growth Design*, 2021, **21**, 4055.
 S101 R. Azumi, G. Gotz, T. Debaerdemaeker and P. Bauerle, *Chem. Eur. J.*, 2000, **6**, 735.
 S102 R. Azumi, E. Mena-Osteritz, R. Boese, J. Benet-Buchholz and P. Bauerle, *J. Mater.*

- Chem.*, 2006, **16**, 728.
- S103 M. A. Neumann, C. Tedesco, S. Destri, D. R. Ferro and W. Porzio, *J. Appl. Crystallogr.*, 2002, **35**, 296.
- S104 H. Pan, P. Liu, Y. Li, Y. Wu, B. S. Ong, S. Zhu and G. Xu, *Adv. Mater.*, 2007, **19**, 3240.
- S105 E. K. Burnett, B. P. Cherniawski, S. J. Rosa, D.-M. Smilgies, S. Parkin and A. L. Briseno, *Chem. Mater.*, 2018, **30**, 2550.
- S106 L. Zhang, N. S. Colella , F. Liu , S. Trahan , J. K. Baral , H. H. Winter , S. C. B. Mannsfeld and A. L. Briseno, *J. Am. Chem. Soc.*, 2013, **135**, 844.
- S107 J. Takeya, M. Yamagishi, Y. Tominari, R. Hirahara, Y. Nakazawa, T. Nishikawa, T. Kawase, T. Shimoda and S. Ogawa, *Appl. Phys. Lett.*, 2009, **90**, 102120.
- S108 There is an estimation where the transfer integral along the non-parallel direction is one fifth of the stacking direction,^{S109} though the estimation by the photoelectron spectroscopy suggests a smaller value.^{S110}
- S109 L. Ji, J. Fan, G. Qin, N. Zhang, P. Lin and A. Ren, *J. Phys. Chem. C.*, 2018, **122**, 21226.
- S110 Y. Nakayama, Y. Uragami, S. Machida, K. R. Koswattage, D. Yoshimura, H. Setoyama, T. Okajima, K. Mase and H. Ishii, *Appl. Phys. Exp.* 2012, **5**, 11601.
- S111 H. Kobayashi, A. Kobayashi, Y. Sasaki, G. Saito and H. Inokuchi, *Bull. Chem. Soc. Jpn.*, 1986, **59**, 301.